

NASA-CR-3814 19840020680

NASA Contractor Report 3814

# Three-Dimensional Transonic Potential Flow About Complex Three-Dimensional Configurations

Theodore A. Reyhner

JULY 1984

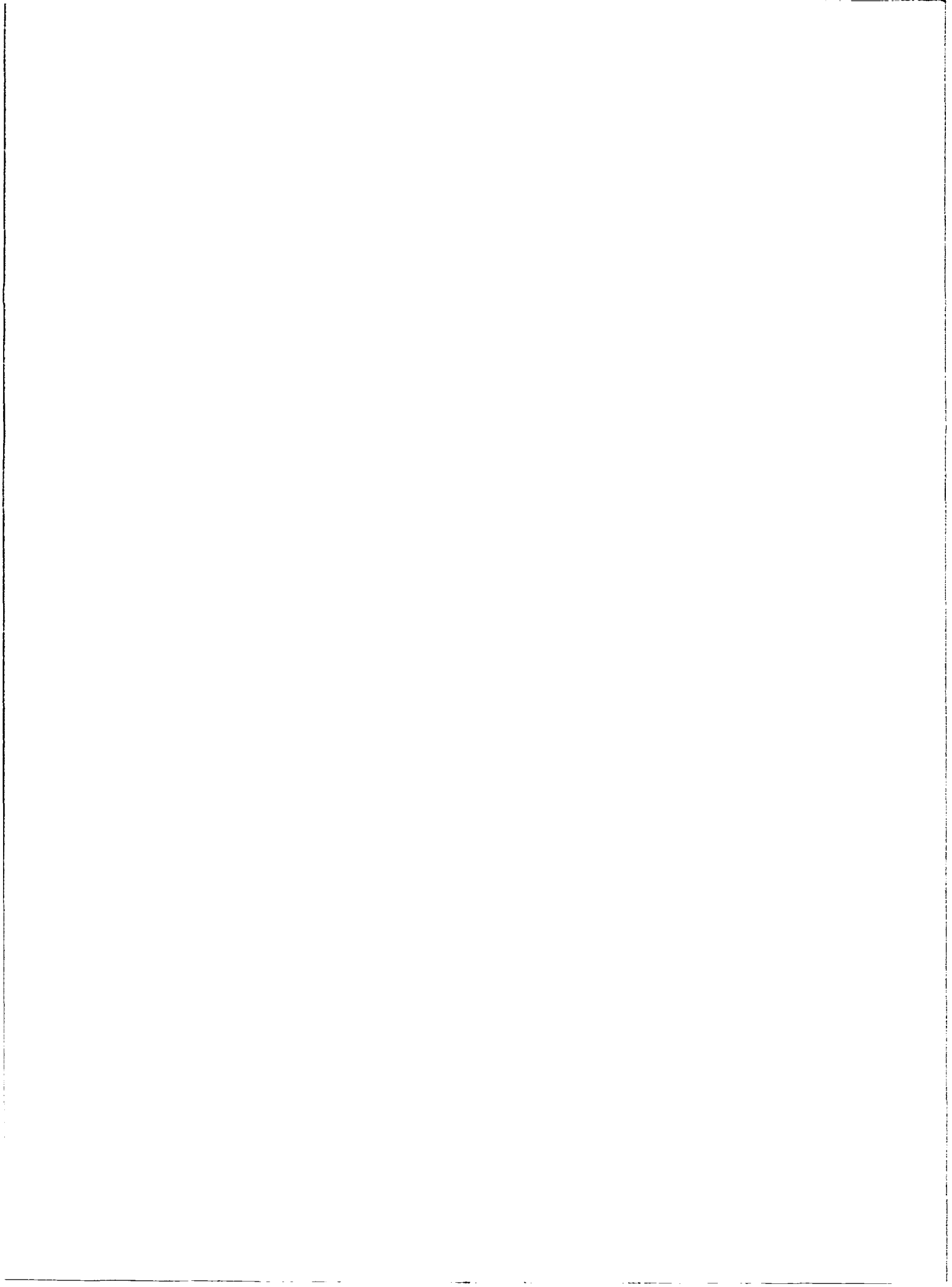
LIBRARY COPY

JUL 19 1984

LINGLY RESEARCH CENTER  
LIBRARY, NASA  
HAMILTON, VIRGINIA

FOR REFERENCE

NOT TO BE TAKEN FROM THIS ROOM



NASA Contractor Report 3814

# Three-Dimensional Transonic Potential Flow About Complex Three-Dimensional Configurations

Theodore A. Reyhner  
*Boeing Commercial Airplane Company*  
*Seattle, Washington*

Prepared under Cooperative Agreement  
with NASA Langley Research Center  
and Boeing Commercial Airplane Company



National Aeronautics  
and Space Administration

Scientific and Technical  
Information Branch

1984



# CONTENTS

	Page
1.0 SUMMARY .....	1
2.0 INTRODUCTION .....	2
3.0 NOMENCLATURE .....	3
4.0 ANALYSIS .....	5
4.1 Equation and Boundary Conditions .....	5
4.1.1 Potential Flow Equation .....	5
4.1.2 Boundary Conditions .....	7
4.2 Kutta Boundary Condition .....	7
4.3 Multigrid .....	11
4.4 Results .....	13
4.5 Conclusions .....	16
5.0 USE OF THE PROGRAM .....	28
5.1 Input Format .....	28
5.1.1 Summary of Input Groups .....	29
5.1.2 Detailed Input Group Descriptions .....	30
5.1.3 Limits and Timing .....	40
5.1.4 Sample Inputs .....	41
5.2 Input Recommendations .....	45
5.3 Program Output .....	50
5.3.1 Description of Printed Output .....	51
5.3.2 Sample Output .....	51
5.4 Diagnostics and Troubleshooting .....	51
5.4.1 Incorrect Input Other Than Geometry .....	51
5.4.2 Geometry Errors .....	63
5.4.3 Code Failures .....	68
5.4.4 Other Problems .....	68
REFERENCES .....	70

## TABLES

		Page
1	Program Internal Limitations . . . . .	41
2	Standard Inlet Mesh (Level 2) . . . . .	49
3	Headings for Surface Point and Surface Geometry Printout . . . . .	52
4	Convergence History Headings . . . . .	52
5	Surface Point Printout Headings . . . . .	53
6	Field Point Printout Headings . . . . .	53
7	Headings for Kutta Boundary Condition Printout . . . . .	54

## FIGURES

		Page
1	Airplane Coordinate System . . . . .	6
2	Geometry and Boundary Conditions for Inlet Flowfield Computation in Cylindrical Coordinates . . . . .	8
3	Flowfield and Mesh About a Trailing Edge, $y = y_j$ . . . . .	10
4	Turboprop Nacelle Computation . . . . .	14
5	Comparison of Experiment With Analysis for Flow in a Turboprop Inlet Diffuser . . . . .	15
6	NACA-0012 Airfoil, $M_\infty = 0.75$ , Angle of Attack = 1.0 deg . . . . .	17
7	NASA-Langley Wing-Pylon-Nacelle Test Model — Location of Pressure Measurements Used for Analysis Comparison . . . . .	18
8	NASA Wing, Pylon, and Nacelle Model, $M_\infty = 0.2$ , Angle of Attack = 5.0 deg, Configuration 5, $D = 4.5$ in. . . . .	19
	(a) Wing Surface Mach Number, $y/D=0.5$ . . . . .	19
	(b) Pylon Surface Mach Number . . . . .	20
	(c) Nacelle Surface Mach Number . . . . .	21
9	NASA Wing, Pylon and Nacelle Model, $M_\infty = 0.6$ , Angle of Attack = 3.0 Degrees, Configuration 5, $D = 4.5$ in. . . . .	22
	(a) Wing Surface Mach Number, $y/D=0.5$ . . . . .	22
	(b) Pylon Surface Mach Number . . . . .	23
	(c) Nacelle Surface Mach Number . . . . .	24
10	NASA Wing, Pylon, and Nacelle Model, $M_\infty = 0.8$ , Angle of Attack = 2.0 deg, Configuration 5, $D = 4.5$ in. . . . .	25
	(a) Wing Surface Mach Number, $y/D=0.5$ . . . . .	25
	(b) Pylon Surface Mach Number . . . . .	26
	(c) Nacelle Surface Mach Number . . . . .	27

## FIGURES (Concluded)

	Page
11 Part of Input File for Inlet Geometry Data Case . . . . .	42
12 Part of Input File for NACA-0012 Airfoil Analysis . . . . .	43
13 Part of Input File for Wing-Pylon-Nacelle Geometry . . . . .	44
14 Mesh Density Required to Resolve Geometry Effects on Flowfield . . . . .	46
(a) Insufficient Mesh . . . . .	46
(b) Sufficient Mesh . . . . .	46
15 Mesh Spacing Control . . . . .	47
(a) Poor Spacing . . . . .	47
(b) Recommended Mesh Spacing Variation . . . . .	47
16 Standard Inlet Mesh (Coarse) . . . . .	48
17 Sample Program Output . . . . .	55
(a) Sample Output . . . . .	55
(b) Sample Output (Continued) . . . . .	56
(c) Sample Output (Continued) . . . . .	57
(d) Sample Output (Continued) . . . . .	58
(e) Kutta Boundary Condition Geometry Tables . . . . .	59
(f) Sample of Convergence History . . . . .	59
(g) Kutta Boundary Condition $\Gamma$ Table . . . . .	60
(h) Sample of Surface Properties Printout . . . . .	61
(i) Convergence History . . . . .	62
18 Possible Geometry Configurations and Errors . . . . .	64
(a) Surface Points Not Adjacent to Mesh Nodes (Nonpoints) . . . . .	64
(b) Two Points Adjacent to the Same Mesh Node . . . . .	64
(c) Two Points Adjacent to the Same Mesh Node . . . . .	64
19 ISURFTP() $=2$ Points and Possible Problems . . . . .	65
(a) ISURFTP() $=2$ Point, Mesh Node and Surface Coincide . . . . .	65
(b) Almost ISURFTP() $=2$ Points . . . . .	65
(c) ISURFTP() $=2$ Point ( $S_1$ ) and Point ( $S_2$ ) Adjacent to ISURFTP() $=2$ Point . . . . .	65
20 Geometry for BITSET, BITSET1 and BITSET2 Explanations . . . . .	67
(a) Sample Geometry for BITSET1 and BITSET2 Error Explanation . . . . .	67
(b) Sample Geometry for BITSET Error Explanation . . . . .	67
21 Very Coarse Mesh . . . . .	69





## 1.0 SUMMARY

An analysis has been developed for the solution of the full three-dimensional potential flow equation for subsonic or transonic potential flowfields about arbitrary configurations. This analysis is an extension of an earlier analysis to more complex geometries and to lifting surfaces. Possible configurations include inlets, nacelles, nacelles with ground planes, S-ducts, turboprop nacelles, wings, and wing-pylon-nacelle configurations.

The solution procedure is to use an arbitrary mesh and difference quotients to create a system of nonlinear finite-difference equations. The grids used are Cartesian and cylindrical. The difference equations consist of a very large system of algebraic equations. They are solved iteratively by using the initial guess or the results of the previous iteration to linearize and partly decouple the equations. Successive line over-relaxation (SLOR) is used along horizontal, vertical, or alternating horizontal and vertical lines. A sequence of grids is used in combination with multigrid to improve convergence efficiency.

The analysis has been programmed in FORTRAN for the CRAY-1 computer and in extended FORTRAN for the Control Data Corporation Cyber 203 computer. The computer code has been written to obtain maximum performance benefit from the vector operations capability of these computers. Included in this report are descriptions of the input and output files for the computer program.

Comparisons of the analysis results with experimental measurements are presented for several configurations.

## 2.0 INTRODUCTION

This report is a description of an analysis and computer code for the prediction of three-dimensional transonic potential flow about three-dimensional configurations. The program can handle a variety of geometries including lifting surfaces. Configurations include inlets, nacelles, nacelles with ground planes, S-ducts, turboprop nacelles, wings, and wing-pylon-nacelle combinations. The analysis and computer code are extensions of an earlier work (refs. 1 and 2). Extensions include multigrid for a more efficient solution process, greater geometric flexibility, and a Kutta boundary condition to handle wing or wing-like surfaces.

The basic approach is described in detail in Reference 1. In summary, the analysis solves the full compressible potential equation. Either cylindrical or Cartesian coordinates may be used. The analysis does not use a body-fitted grid, so there are no grid generation problems. The partial differential equations are replaced by finite-difference equations which are solved on a grid using successive line over-relaxation (SLOR). Horizontal lines, vertical lines, or alternating horizontal and vertical lines may be used. A sequence of grids is used to calculate the solution using what is commonly referred to as multigrid (ref. 3).

This document covers the use of multigrid, the logic for handling lifting surfaces, and a guide to using this version of the code. Also included are some examples computed using this version of the code.

### 3.0 NOMENCLATURE

a	speed of sound
$C_1, C_2, C_3$	difference quotient coefficients
$C_p$	coefficient of pressure, $(p/p_\infty - 1) / \left( \frac{1}{2} \gamma M_\infty^2 \right)$
D	discrepancy
$F, \bar{F}$	right-hand side of equation
$I, \bar{I}$	interpolation/extrapolation operators
L	differential operator
M	Mach number
$\bar{n}$	unit normal to surface oriented into flowfield
$n_x, n_y, n_z$ , or $n_x, n_r, n_\theta$	components of $\bar{n}$
p	static pressure
q	velocity, $u^2 + v^2 + w^2$ , or $u^2 + u_r^2 + u_\theta^2$
r	radius
$r_{\max}$	r at outer edge of computational cylinder
s	arc length
u	axial velocity component, $u = \phi_x$
$u_r$	radial velocity component, $u_r = \phi_r$
$u_s$	component of velocity along cut of surface
$u_\theta$	circumferential velocity component, $u_\theta = \frac{1}{r} \phi_\theta$
v	velocity component in y direction, $v = \phi_y$
w	velocity component in z direction, $w = \phi_z$
x	axial coordinate
y	coordinate, y
z	coordinate, z

## NOMENCLATURE (Concluded)

$\alpha$	flow angle
$\gamma$	ratio of specific heats
$\Gamma$	$\Delta\phi$ for Kutta boundary condition jump
$\Delta x, \Delta y, \dots$	step size in x, y, etc.
$\Delta\phi$	change in $\phi$
$\theta$	circumferential coordinate, $\arctan(y/z)$
$\phi$	potential function
$\phi_{(n)}^k$	$\phi$ at sweep n for grid k
$\phi_n$	velocity normal to surface
$\phi_s$	$\partial\phi/\partial s$ , velocity in direction of s
$\Phi$	exact solution for $\phi$
$\omega_x, \omega_y, \dots$	over-relaxation parameters for x, y, etc.
<b>Subscript</b>	
i	index for x mesh values
j	index for y mesh values
k	index for z mesh values or grid number
A, A'	surface points
S, S <sub>1</sub> , S <sub>2</sub>	surface points
x, y, z, r, $\theta$ , s	partial derivatives
$\infty$	freestream
<b>Superscripts</b>	
k	grid number
<b>Special</b>	
$\phi_z _k$	$\phi_z$ at point i, j, k
$\phi_{F-k}^{k-1}$	$\phi$ on grid k-1 obtained by interpolation from grid k

## 4.0 ANALYSIS

The full partial differential equation for compressible transonic flow expressed in terms of a velocity potential,  $\phi$ , is solved by replacing the partial derivatives with difference quotients. The difference quotients are formed using values of the potential at the discrete nodes formed by the intersection of a network of Cartesian or cylindrical grid lines with each other and the surface. The grid used is not body-fitted. When the partial derivatives are replaced with difference quotients, a nonlinear difference equation is obtained at each grid intersection in the flowfield. The difference equations form a large system of algebraic nonlinear equations which are not practical to solve directly. The solution of the difference equations is obtained by approximating the system of equations by a linear system and solving that system using successive line over-relaxation (SLOR). This process is iterated until convergence. The formulas for the difference quotients and the resulting difference equations are covered in Reference 1. This analysis differs from Reference 1 in that Cartesian coordinates can be used as well as cylindrical coordinates.

The primary difference between this analysis and that of Reference 1 is the way a sequence of grids is used to calculate the solution to the equations on the finest grid. The basic difficulty with using SLOR to solve a large system of difference equations such as these is that the convergence rate is very slow for fine meshes. An estimate or starting guess for the solution can be computed using coarse meshes, but relaxing the starting solution to a final solution on a fine mesh still takes a considerable number of sweeps. This code uses the multigrid technique which uses the coarse grids to correct the fine grid solution. This greatly reduces the number of cycles required on the fine mesh and the overall work required.

The logic for calculating lift about wing-like surfaces is also included in this version of the analysis.

### 4.1 EQUATION AND BOUNDARY CONDITIONS

The equation to be solved is the complete equation for inviscid, irrotational flow formulated in terms of a velocity potential,  $\phi$ . The Cartesian coordinate system is shown in Figure 1.

#### 4.1.1 POTENTIAL FLOW EQUATION

The equation for the velocity potential in Cartesian coordinates is

$$(a^2 - \phi_x^2)\phi_{xx} + (a^2 - \phi_y^2)\phi_{yy} + (a^2 - \phi_z^2)\phi_{zz} - 2\phi_x\phi_y\phi_{xy} - 2\phi_y\phi_z\phi_{yz} - 2\phi_z\phi_x\phi_{zx} = 0 \quad (1)$$

where  $\phi$  is the velocity potential and the local speed of sound,  $a$ , is given by

$$a^2 = a_\infty^2 - \frac{\gamma-1}{2} (\phi_x^2 + \phi_y^2 + \phi_z^2 - q_\infty^2). \quad (2)$$

The velocity components in the flowfield ( $u$ ,  $v$ ,  $w$ ) are obtained from the potential function with the following relationships:

$$\begin{aligned} u &= \phi_x, \\ v &= \phi_y, \\ w &= \phi_z, \end{aligned} \quad (3)$$

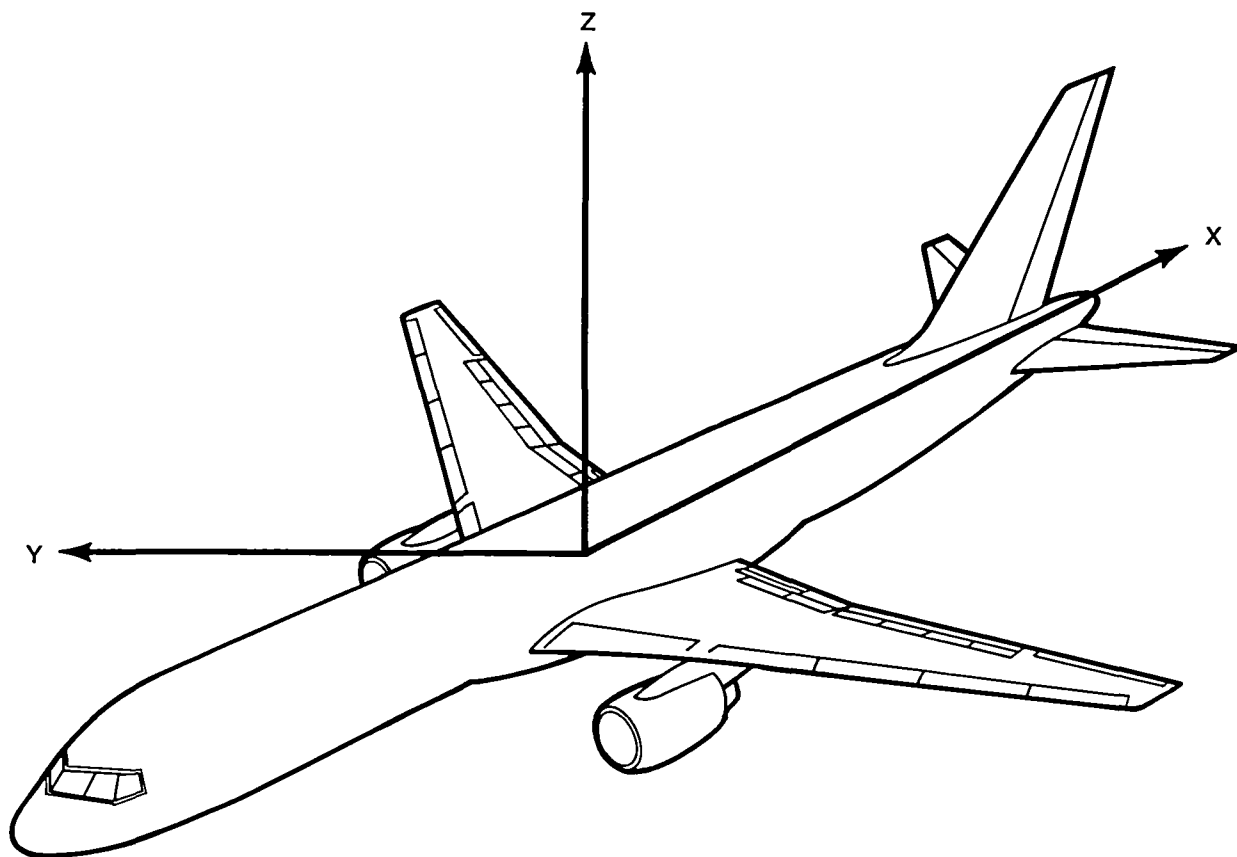


*Figure 1. Airplane Coordinate System*

The potential equation in cylindrical coordinates (fig. 2) is

$$\begin{aligned} & (a^2 - \phi_x^2)\phi_{xx} + (a^2 - \phi_r^2)\phi_{rr} + \left(a^2 - \frac{\phi_\theta^2}{r^2}\right)\frac{\phi_{\theta\theta}}{r^2} - \\ & - 2\phi_x\phi_r\phi_{xr} - 2\phi_r\phi_\theta\frac{\phi_{r\theta}}{r^2} - 2\phi_\theta\phi_x\frac{\phi_{\theta x}}{r^2} + \left(a^2 + \frac{\phi_\theta^2}{r^2}\right)\frac{\phi_r}{r} = 0. \end{aligned} \quad (4)$$

This is similar to the equation in Cartesian coordinates and the solution technique is the same. The axis points are special and the analysis for the axis is described in Reference 1. The coordinates are related by:

$$\begin{aligned} y &= r \cos \theta \\ z &= r \sin \theta \end{aligned} \quad (5)$$

and

$$\begin{aligned} u_r &= \phi_r = v \cos \theta + w \sin \theta \\ u_\theta &= \frac{\phi_\theta}{r} = -v \sin \theta + w \cos \theta. \end{aligned} \quad (6)$$

#### 4.1.2 BOUNDARY CONDITIONS

The boundary condition at solid surfaces is that the velocity normal to the surface,  $\phi_n$ , equals zero. The boundary condition at the exit of a duct, or at the compressor face of an inlet, is that the axial velocity is fixed at the uniform value that gives a specified mass flow. At the left (inflow) boundary of the computational field, the potential function,  $\phi$ , is specified. At the left boundary,

$$\phi = u_\infty x + v_\infty y + w_\infty z + \text{constant}. \quad (7)$$

At the right boundary of the flowfield the outflow velocity,  $u = \phi_n$ , is specified. At the sides of the flowfield, for Cartesian coordinates, the outflow velocities,  $v$  or  $w = \phi_n$ , are specified. When cylindrical coordinates are used, the outflow velocity is specified on the top half of the cylinder ( $\theta < 90$  deg and  $\theta > 270$  deg) and equation (7) is used to specify  $\phi$  on the bottom half ( $90$  deg  $\leq \theta \leq 270$  deg) (fig. 2).

The choice of boundary conditions is not unique. Whether a velocity normal to the surface or  $\phi$  is specified is a matter of choice except for the compressor face or duct exit. It is not possible to prescribe freestream velocity at the outer boundaries as that would be too many boundary conditions. Specifying  $\phi$  at the boundary enforces the tangential velocity component and specifying  $\phi_n$  enforces the normal component of the velocity. This is satisfactory as long as the boundaries are placed far enough from the object of interest. Five to ten diameters out appears to be satisfactory for inlet and nacelle computations.

#### 4.2 KUTTA BOUNDARY CONDITION

The analysis of flows about lifting surfaces (wings) requires a means to compute a solution with circulation. The magnitude of the circulation is determined by applying the Kutta condition at the trailing edge of the lifting surface. A jump or discontinuity is required in the potential at some point in the flowfield in order to have circulation.

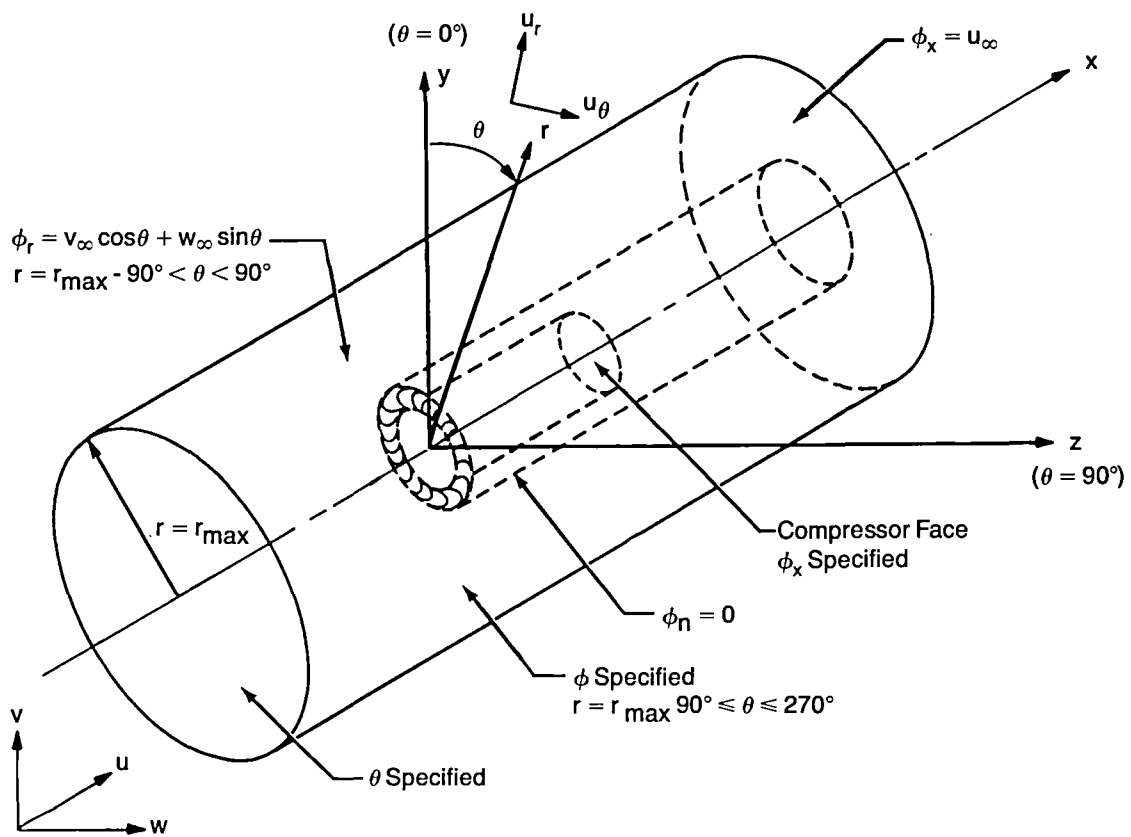


Figure 2. Geometry and Boundary Conditions for Inlet Flowfield Computation in Cylindrical Coordinates



The discontinuity in the potential for this analysis is taken as a cut in the flowfield extending straight back in  $x$  from the trailing edge of the lifting surface. At any trailing edge point on the surface a jump in the potential across the cut is computed and that jump value is applied whenever difference quotients are computed using points on both sides of the discontinuity surface. The jump value is held constant downstream of the trailing edge but can vary in the spanwise direction.

The jump in the potential,  $\Gamma_j$ , is determined by applying the Kutta condition, which requires that the trailing edge point be a stagnation point in the flowfield (two-dimensional flow). With the nonbody-fitted mesh, there is, in general, no mesh-surface intersect on the exact trailing edge and, thus, the Kutta condition must be applied in an approximate manner. The criterion used requires no flow around the trailing edge.

Referring to Figure 3 for notation  $\phi_{\text{upper}}$  is defined as the potential function  $\phi$  above the cut and  $\phi_{\text{lower}}$  as the potential function  $\phi$  below the cut. Then

$$\phi_{\text{upper}} = \phi_{\text{lower}} + \Gamma_j \quad (8)$$

where  $j$  is the index of the  $y$  mesh for the cross-section shown. The velocity of the flow about the trailing edge can be defined using either  $\phi_{\text{upper}}$  or  $\phi_{\text{lower}}$ . Using  $\phi_{\text{upper}}$  this velocity is defined by

$$\phi_s|_{\text{trailing edge}} = \frac{\phi_{\text{upper}|_A} - \phi_{\text{upper}|_{A'}}}{\Delta s} \quad (9)$$

The condition that  $\phi_s$  at the trailing edge equals zero gives

$$\phi_{\text{upper}|_A} = \phi_{\text{upper}|_{A'}} \quad (10)$$

What is computed and stored is  $\phi_{\text{upper}}$  above the cut and  $\phi_{\text{lower}}$  below the cut. Thus, equation 10 becomes

$$\phi_{\text{upper}|_A} = \phi_{\text{lower}|_{A'}} + \Gamma_j \quad (11)$$

$\Gamma_j$  is computed by setting

$$\Gamma_j = \phi|_A - \phi|_{A'} \quad (12)$$

where the subscripts upper and lower have been dropped.  $\phi = \phi_{\text{upper}}$  above the cut and  $\phi_{\text{lower}}$  below the cut.

Once the jump,  $\Gamma_j$ , is computed, it is used in the calculation of any difference quotients representing  $z$  derivatives that involve points on both sides of the flowfield discontinuity or cut. Since three-point derivatives are used, it is the difference quotients for  $k$  and  $k-1$  that are affected. As an example, if the standard difference quotient for  $\phi_z$  at  $k$  is given by

$$\phi_z|_k = C_1\phi_{k+1} + C_2\phi_k + C_3\phi_{k-1}, \quad (13)$$

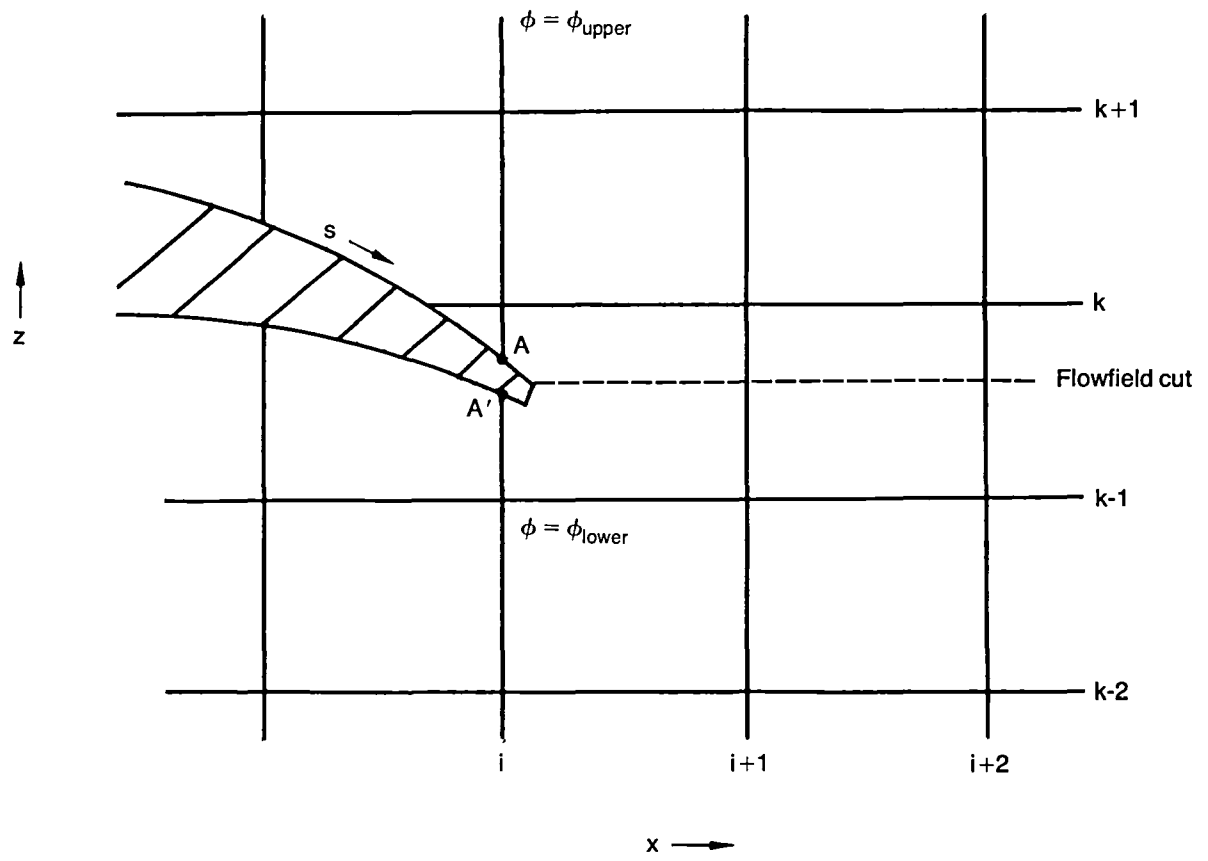


Figure 3. Flowfield and Mesh About a Trailing Edge,  $y = y_j$

then when the discontinuity is present between  $k$  and  $k-1$ ,

$$\phi_{z|k} = C_1\phi_{\text{upper}|_{k+1}} + C_2\phi_{\text{upper}|_k} + C_3\phi_{\text{upper}|_{k-1}} \quad (14)$$

is the correct formula except that  $\phi_{\text{upper}}$  is not what is saved at  $k-1$ . However, the formula can be rewritten as

$$\phi_{z|k} = C_1\phi_{\text{upper}|_{k+1}} + C_2\phi_{\text{upper}|_k} + C_3\left(\phi_{\text{lower}|_{k-1}} + \Gamma_j\right) \quad (15)$$

which can be again rewritten

$$\phi_{z|k} = C_1\phi_{k+1} + C_2\phi_k + C_3\phi_{k-1} + C_3\Gamma_j. \quad (16)$$

Thus, the jump creates a correction  $C_3\Gamma_j$  to the usual formula for the difference quotient. It can be shown that

$$\phi_{z|_{k-1}} = C_1\phi_k + C_2\phi_{k-1} + C_3\phi_{k-2} - C_1\Gamma_j \quad (17)$$

where for this equation  $C_1$ ,  $C_2$ , and  $C_3$  are the appropriate coefficients at  $k-1$ .

### 4.3 MULTIGRID

The multigrid procedure is an algorithm for solving the finite-difference equations. It is used in conjunction with the successive line over-relaxation (SLOR) technique to accelerate (in terms of number of sweeps and quantity of computational work) the convergence of the solution to the finite-difference equations. Theoretically, for some problems, very great reductions in computational work are possible.

In simplest terms, multigrid allows corrections to a solution being computed on a fine mesh to be computed using a coarser mesh. Computations on a coarser mesh are less expensive because there are fewer points and larger corrections to the solution per sweep are possible. The theory of multigrid (again in simpler terms, see References 3 and 4 for greater detail) is based on the error in a solution consisting of a variety of wavelengths. On a given mesh the error components with wavelengths of the order of the mesh spacing are reduced or eliminated quickly, that is, in a small number of sweeps. The error components with long wavelengths, those many times the mesh spacing, are reduced very slowly, and this is the primary difficulty with standard relaxation techniques. Multigrid uses a sequence of meshes and, in its pure form, every wavelength is eliminated on a mesh where it is of the order of the mesh spacings. Hence, very few sweeps are required on each mesh. For linear problems, the entire theory is relatively straightforward. For nonlinear problems, the theory is more complex. Success of multigrid depends on many things. One critical item is that sweeping on the fine mesh does indeed eliminate the high-frequency error terms, that is, smooth the error. The mesh aspect ratio does affect this item. Another factor is how the boundary points are processed. Both these items probably adversely affect the efficiency of the multigrid scheme in this code.

The finite-difference equation set can be written as

$$L^k(\phi_{(n)}^k; \phi_{(n-1)}^k) = F^k \quad (18)$$

where  $L^k$  is an operator on grid  $k$ ,  $\phi_{(n)}^k$  is the solution matrix at sweep  $n$  on grid  $k$ , and  $F^k$  is independent of  $\phi_{(n)}$  and  $\phi_{(n-1)}$ .  $L^k$  is a linear operator on  $\phi_{(n)}^k$ , but derived from a nonlinear equation which has been linearized by using values of  $\phi^k$  from the previous sweep,  $n-1$ . An exact solution,  $\Phi^k$  on grid  $k$ , is defined by

$$L^k(\Phi^k; \Phi^k) = F^k. \quad (19)$$

An error or discrepancy term,  $D^k$ , can be defined by

$$D_{(n)}^k = L^k(\phi_{(n)}^k; \phi_{(n)}^k) - F^k. \quad (20)$$

What is desired is a correction,  $\Delta\phi^k$ , to the solution,  $\phi_{(n)}^k$ , that reduces the error,  $D^k$ . That is,

$$L^k(\phi_{(n)}^k + \Delta\phi^k; \phi_{(n)}^k + \Delta\phi^k) - F^k \ll D_{(n)}^k. \quad (21)$$

Such a correction can be computed on a coarser mesh, grid  $k-1$ , and the error is reduced if the assumptions made previously are correct.

An injection operator,  $I_k^{k-1}$ , is required to generate an initial field on grid  $k-1$  from that on grid  $k$ . If all the points of grid  $k-1$  are in grid  $k$ , the simplest operator just takes those values from the grid  $k$  solution that corresponds to points in grid  $k-1$ . Then,

$$\phi_{F-k}^{k-1} = I_k^{k-1} \phi_{(n)}^k \quad (22)$$

where  $\phi_{F-k}^{k-1}$  is  $\phi$  on grid  $k-1$  obtained from grid  $k$ .

The error term  $D_{(n)}^k$  can also be injected down to level  $k-1$ , giving us

$$\bar{I}_k^{k-1} D_{(n)}^k \quad (23)$$

on level  $k-1$ . Note that  $\bar{I}$  need not be the same operator as  $I$ . What is desired is a  $\Delta\phi$  calculated on level  $k-1$  which, when added to  $\phi_{F-k}^{k-1}$ , gives an error term on level  $k-1$  equal to  $-\bar{I}_k^{k-1} D_{(n)}^k$ .

This is still not sufficient as even an exact solution  $\Phi^k$  with resulting  $D^k$  equal to 0 will generally lead to an error term on a lower level. That is,

$$L^{k-1}(I_k^{k-1} \Phi^k; I_k^{k-1} \Phi^k) - F^{k-1} \neq 0. \quad (24)$$

The problem to be solved on level  $k-1$  is

$$L^k(\phi_{(m)}^{k-1}; \phi_{(m-1)}^{k-1}) = \bar{F}^{k-1} \quad (25)$$

where

$$\bar{F}^{k-1} = L^{k-1}(\phi_{F-k}^{k-1}; \phi_{F-k}^{k-1}) - \bar{I}_k^{k-1} D_{(n)}^k. \quad (26)$$

Once a solution  $\phi_{(m)}^{k-1}$  is obtained on level k-1, the difference between it and the initial solution on level k-1,  $\phi_{F-k}^{k-1}$ , is expanded to level k using an expansion operator  $I_{k-1}^k$  and added to the previous solution on level k.

$$\phi_{\text{new}}^k = \phi_{\text{last}}^k + I_{k-1}^k (\phi_{(m)}^{k-1} - \phi_{F-k}^{k-1}) \quad (27)$$

The solution on level k-1 can be obtained using levels k-2 and the same technique. Similarly, levels k-3, k-4, etc., can be used in the calculation.

This particular program uses a maximum of four levels. Grid k-1 is obtained from grid k by deleting every other mesh, except for  $\theta$  mesh. With cylindrical coordinates, an option exists for leaving the  $\theta$  mesh unchanged between grids. This is desirable, since for some  $\theta$  meshes, smoothing of the error term in  $\theta$  can be very poor and, hence, the multigrid process can fail if the  $\theta$  mesh varies (ref. 4). Inadequate smoothing in the  $\theta$  coordinate is caused by mesh aspect ratios,  $r\Delta\theta/\Delta x$  and  $r\Delta\theta/\Delta r$ , that are much greater than one. These can occur because for near axisymmetric geometries it is possible to obtain good accuracy with relatively coarse  $\theta$  meshes.

$I_k^{k-1}$  is a straight injection operator used with the potential function  $\phi$ . This gives as the  $\phi$  value in grid k-1 the  $\phi$  value at the same point in grid k. The operator  $\bar{I}_k^{k-1}$  used with  $D^k$  is a volume weighted injection operator so that  $\bar{I}_k^{k-1} D^k$  is a volume weighted average of the  $D^k$  in the immediate vicinity of the grid point. This provides additional smoothing of the error term beyond that of the relaxation scheme. The expansion operator  $I_{k-1}^k$  is a parametric cubic interpolator which uses the function and first derivatives. The first derivatives are calculated on the coarse grid using three-point difference formulas.

Multigrid, as applied to this program, works best for fine meshes. As the mesh becomes coarser, more points involve boundary conditions and the multigrid procedure may not correctly handle the boundary and near boundary points. For very coarse grids there may be only one mesh line between surfaces, and all the field points in a region are adjacent to surfaces. The differencing for such field points is nonstandard, and the multigrid assumptions do not necessarily apply. It is not clear what happens in this situation except that it is certainly adverse.

#### 4.4 RESULTS

This program and its predecessors have been used for several years to calculate inlet and nacelle flowfields. Typical results are shown in References 1 and 2. Good agreement with experiments for inlet calculations can be obtained by using cylindrical meshes with about 50 000 mesh nodes.

Other configurations that have been calculated with the code are flow in the lobe of a multilobe mixer, an inlet in the influence of a ground plane, and flow about a turboprop chin inlet. The turboprop chin inlet required the maximum number of grid points, and even this provided only an approximate flowfield. The difficulty was that the inlet was small relative to the nacelle and spinner and thus a mesh fine enough to resolve the inlet was too fine for the spinner. This problem would benefit greatly from a capability to locally embed a finer mesh or to use larger (and hence, denser) meshes. A wireframe of the geometry, a cross-section for  $y=0.0$ , and computed results are shown in Figure 4.

Another configuration that has been computed is an "S" duct for a turboprop installation such as the one described previously. This configuration included the shaft for the prop and a fairing around the shaft. This calculation was made with about 50 000 mesh nodes and gave good agreement with experimental data (fig. 5).

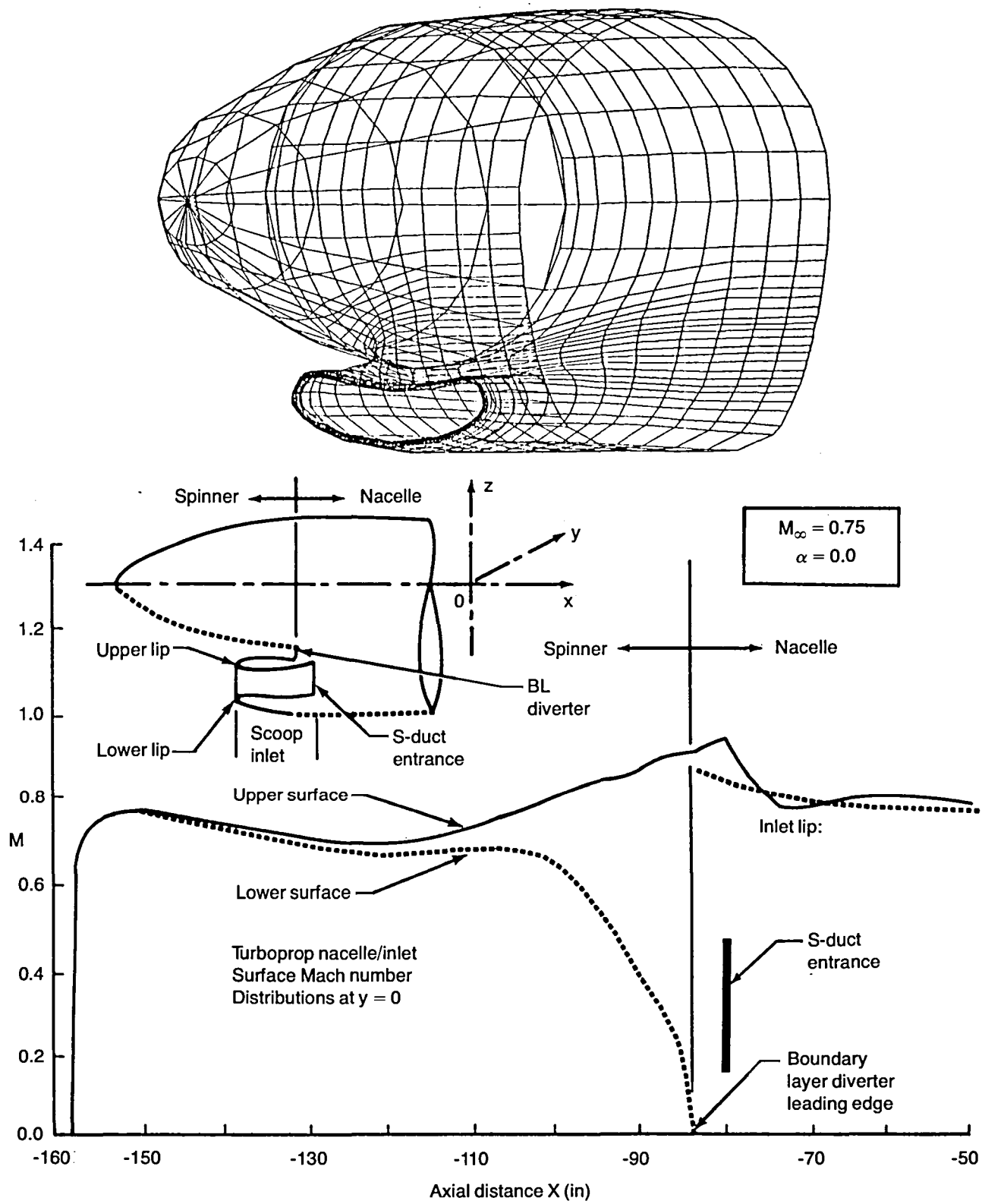


Figure 4. Turboprop Nacelle Computation

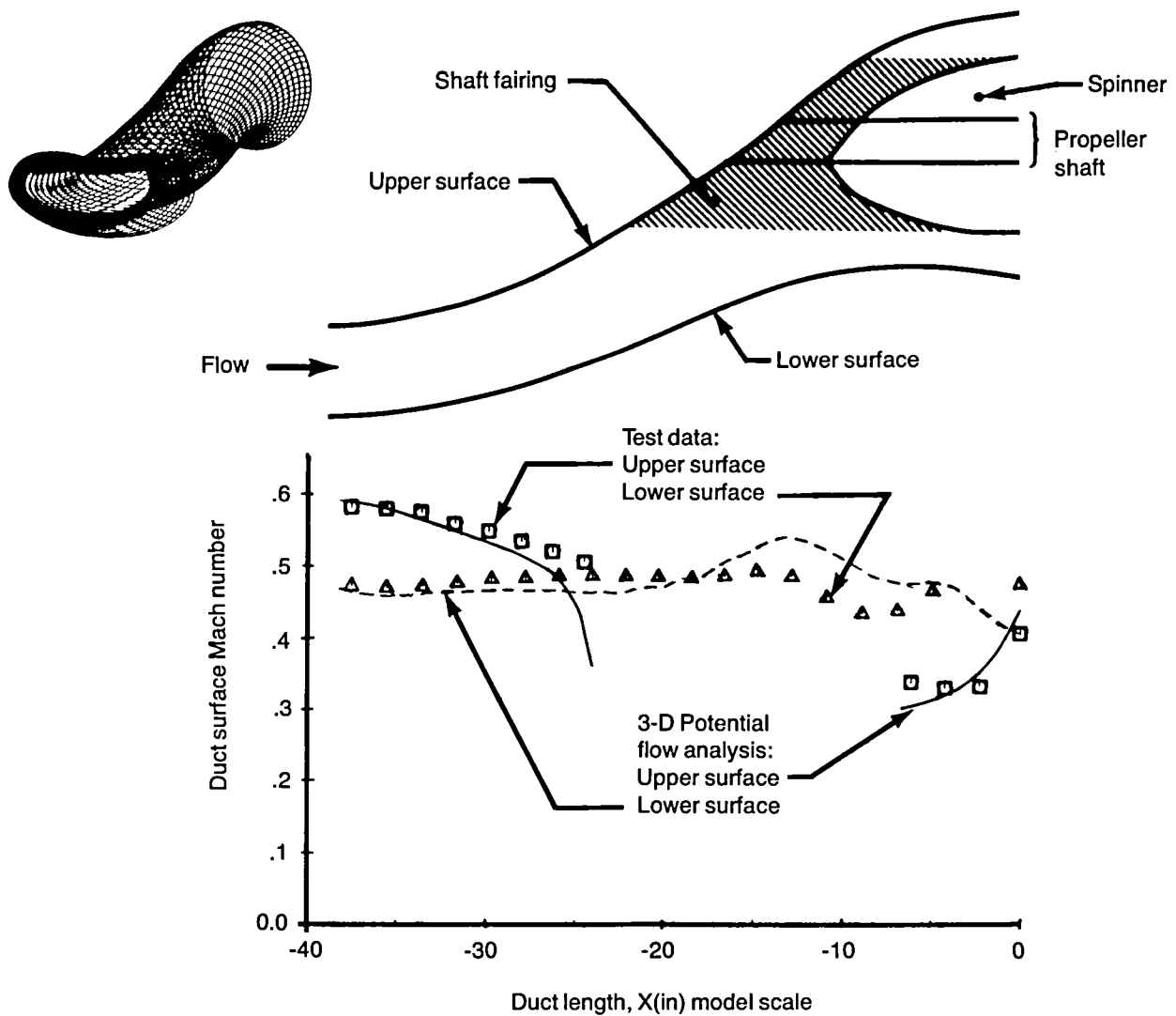


Figure 5. Comparison of Experiment With Analysis for Flow in Turboprop Inlet Diffuser

Several trial calculations were made with 2-D wing configurations to verify that the Kutta condition was properly applied. Figure 6 shows results for an NACA-0012 airfoil at Mach 0.75 and 1-deg angle of attack. Experimental results are from Reference 5. The computation used 35 600 nodes, nine mesh along the wing and 25 mesh chordwise across the wing. Results are excellent. Disagreement with the experiment shown is typical of potential flow results (no boundary-layer effects included). A finer grid would give a better defined (sharper) shock wave.

An attempt was made to compute a solution about the outer nacelle of a 747 including part of the wing and the pylon. Results were unsatisfactory. The primary problem was that the mesh along the wing was too coarse and, hence, the boundary conditions where the wing exited the computational volume could not be enforced properly. The problem was run using 250 000 grid points, the maximum available. Whether this problem could be solved successfully using a denser mesh is not known.

A solution was calculated for a straight wing, pylon, and flow-through nacelle model tested at the NASA-Langley Research Center (ref. 6). The straight two-dimensional wing made the side boundary condition simpler and allowed a coarser mesh to be used successfully. Good agreement with experiment was obtained by using the maximum number of mesh and mesh-surface intersects currently possible and by careful selection of mesh values. Top, front, and side views showing the location of the pressure tap rows used for data comparison are shown in Figure 7. Results are shown in Figures 8 through 10 for free-stream Mach numbers of 0.2, 0.6 and 0.8. The results for the wing upper surface Mach number at a freestream Mach number of 0.8 show an expansion approaching the trailing edge. This is appropriate for supersonic inviscid flow over a convex surface. The trailing edge shock is very strong, so it is reasonable to assume that the wing boundary layer separates and that the differences between experiment and analysis are viscous effects.

The calculations for the wing-pylon-nacelle configuration were made with a compressor face at  $x = -4.1$ , and an extension of the nacelle as a cylinder to the computational boundary. The Mach number at the compressor face was estimated from the data at the nacelle exit. Assuming that the flow at the duct exit was at  $M_\infty$  would give approximately the same solution.

#### 4.5 CONCLUSIONS

The analysis gives good results as long as two criteria are met. First, inviscid irrotational flow has to be the correct model for the flow; that is, boundary layers have to be thin and attached. Second, the geometry and, thus, the flowfield, cannot be too complicated. Flowfield features must be resolved by the mesh and the number of mesh is limited by the size of the core memory of the computer.

The required central processor times for this analysis are quite reasonable. Usually the times are less than five minutes even for 250 000 field points. This is primarily the consequence of using multigrid for the solution procedure, since with multigrid run times are approximately proportional to the number of points. If more memory, with the same computation speed, becomes available, solving for the flowfields about more complex configurations would be practical.



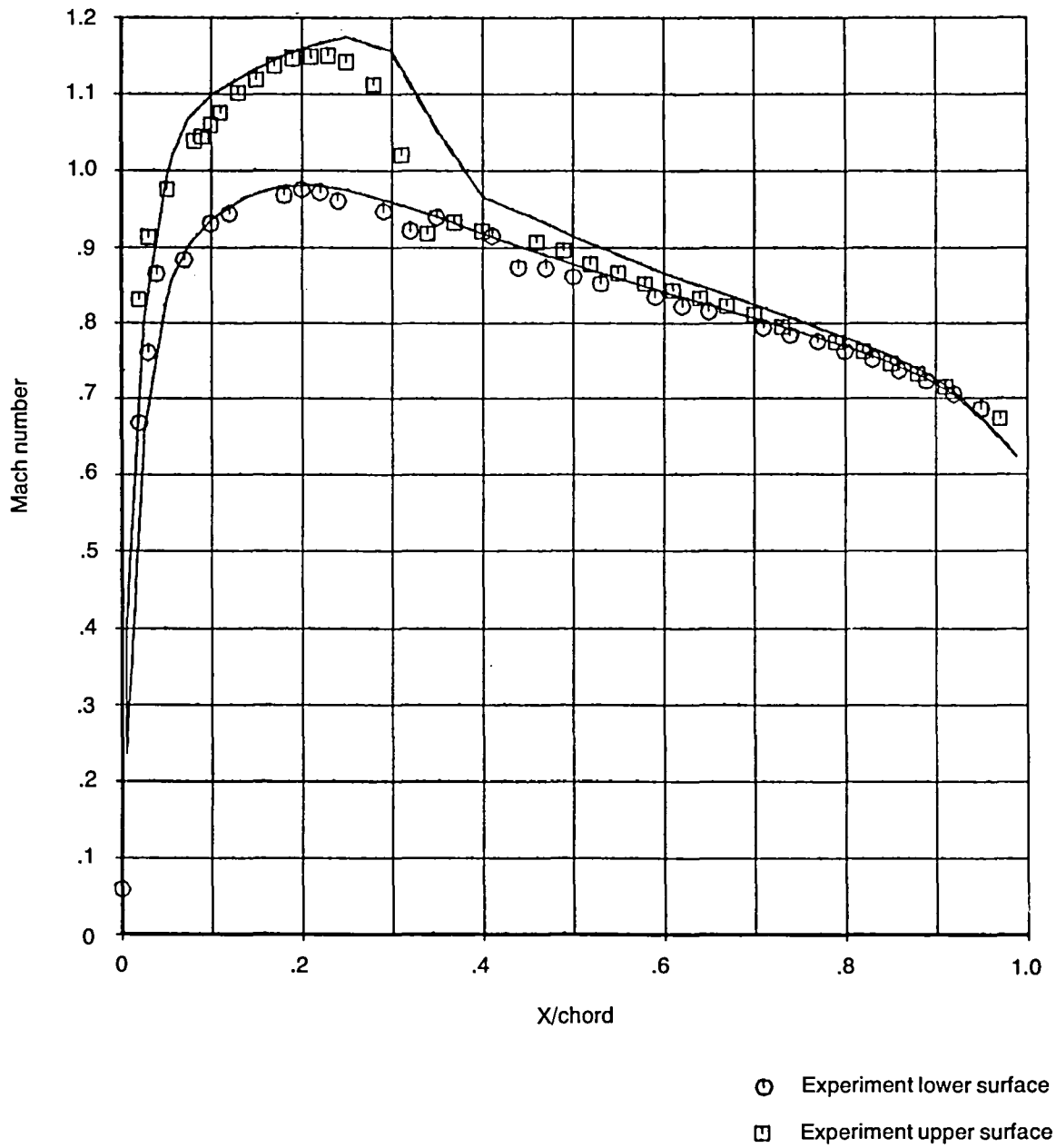


Figure 6. NACA-0012 Airfoil,  $M_\infty = 0.75$ , Angle of Attack = 1.0 deg

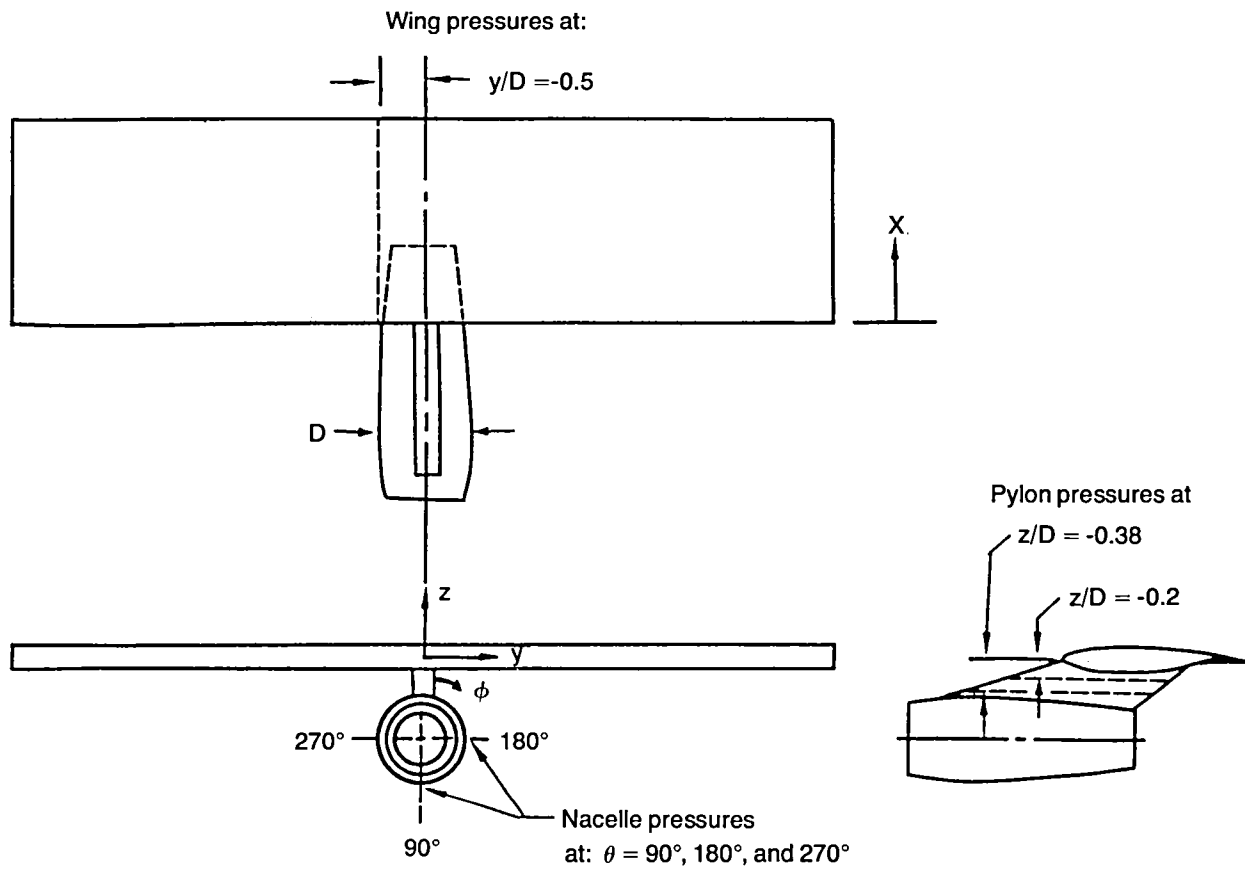
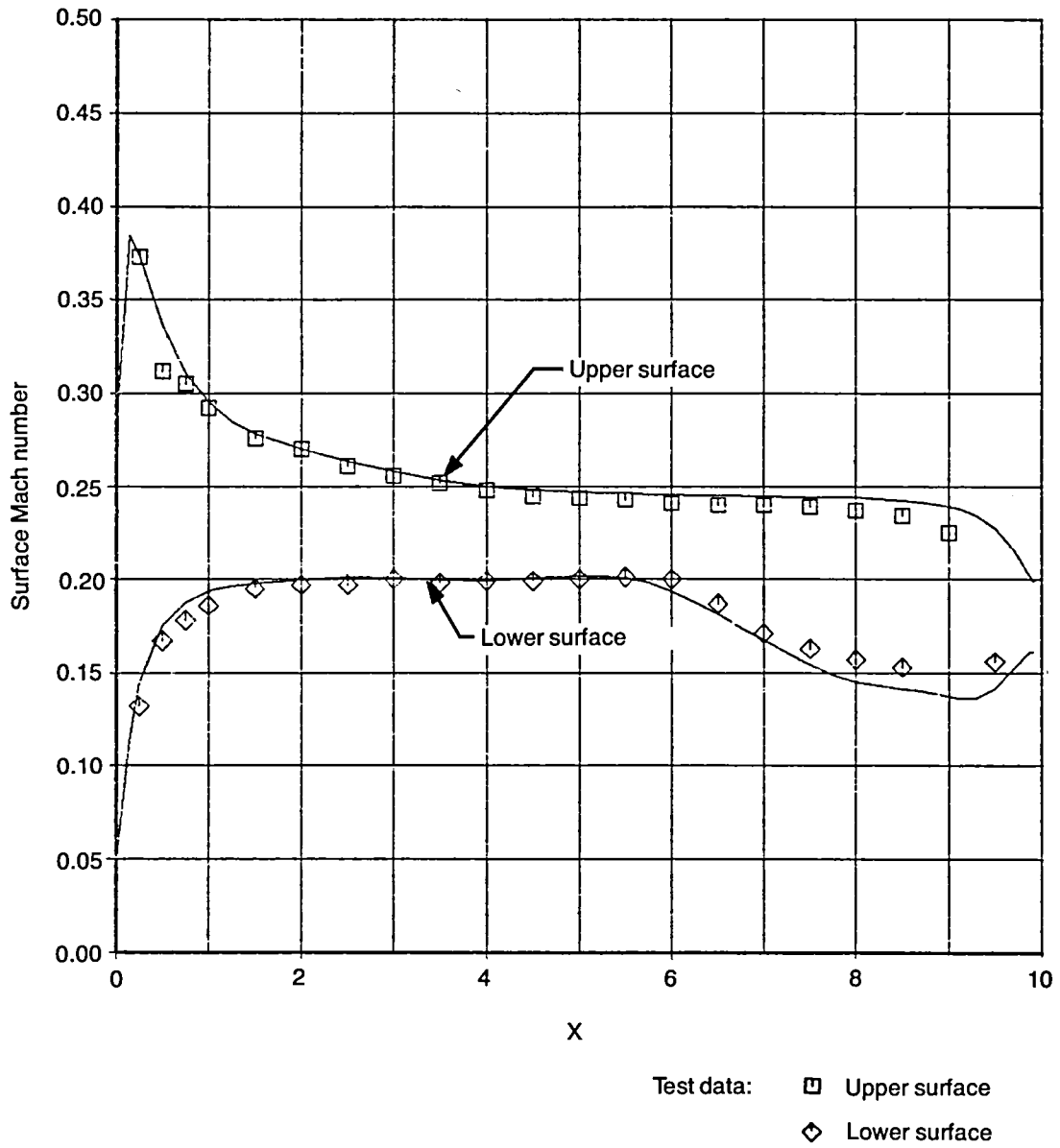
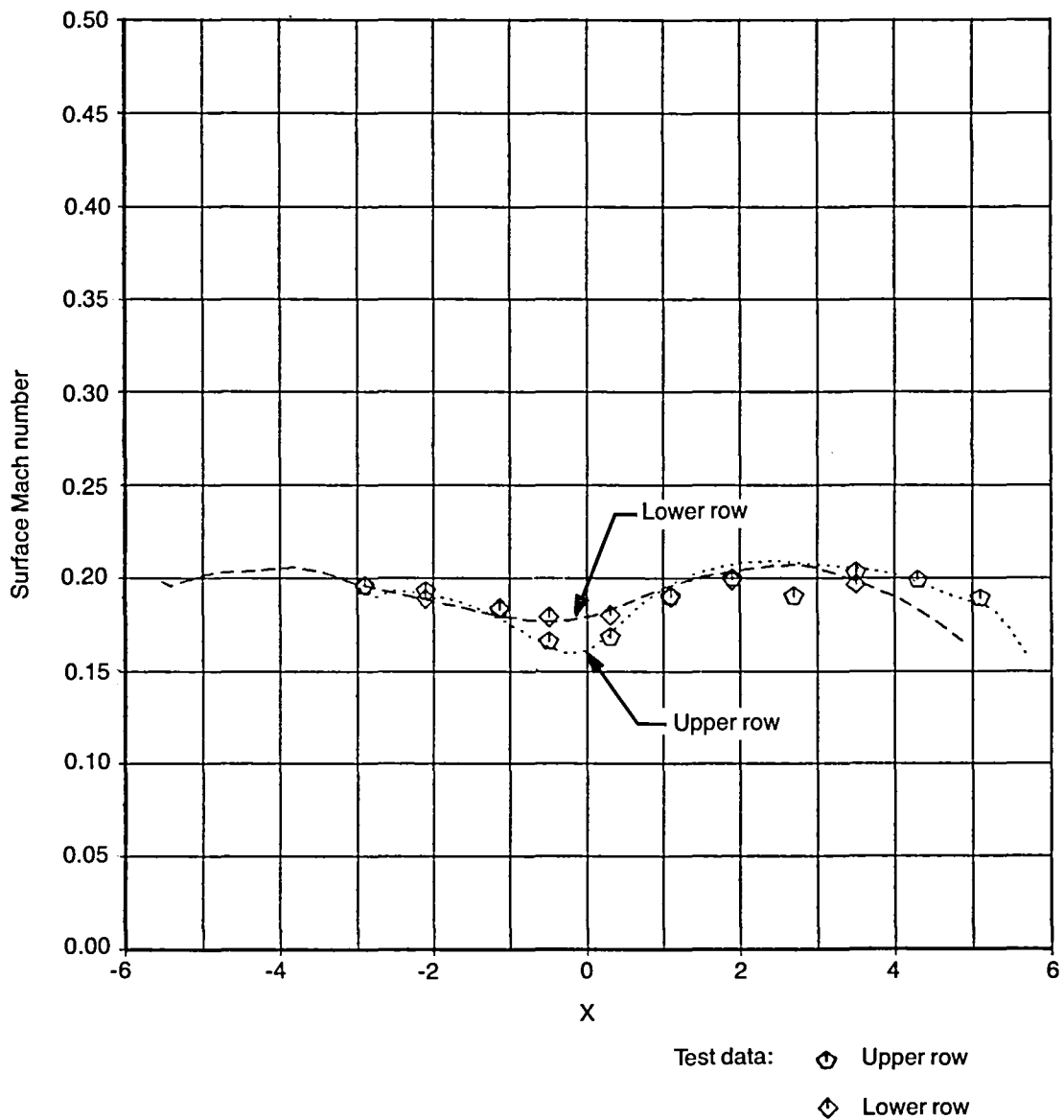


Figure 7. NASA-Langley Wing-Pylon-Nacelle Test Model – Location of Pressure Measurements Used for Analysis Comparison



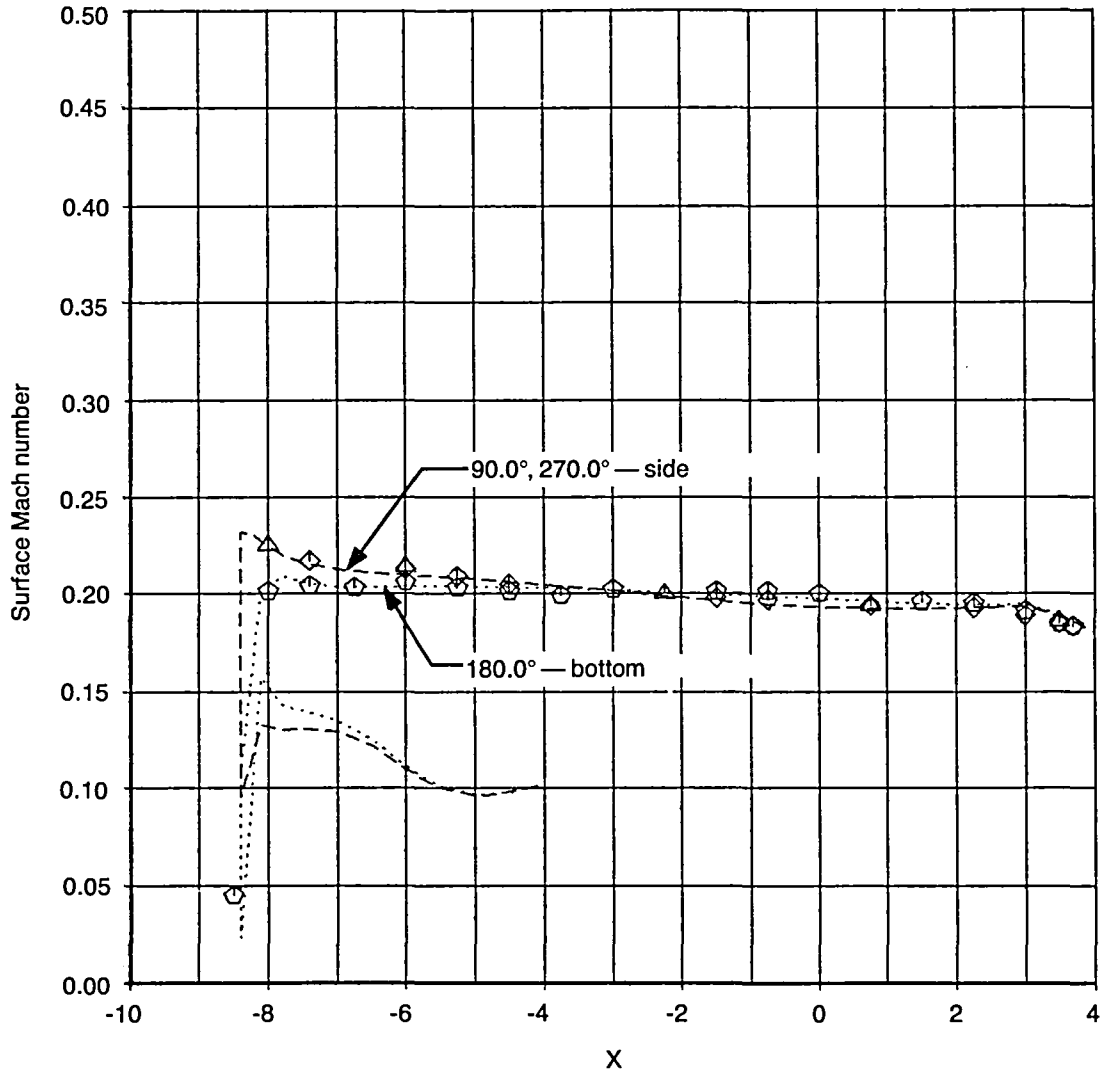
(a) Wing Surface Mach Number,  $y/D = 0.5$

Figure 8. NASA Wing, Pylon, and Nacelle Model,  $M_\infty = 0.2$ , Angle of Attack = 5.0 deg, Configuration 5,  $D = 4.5$  in



(b) Pylon Surface Mach Number

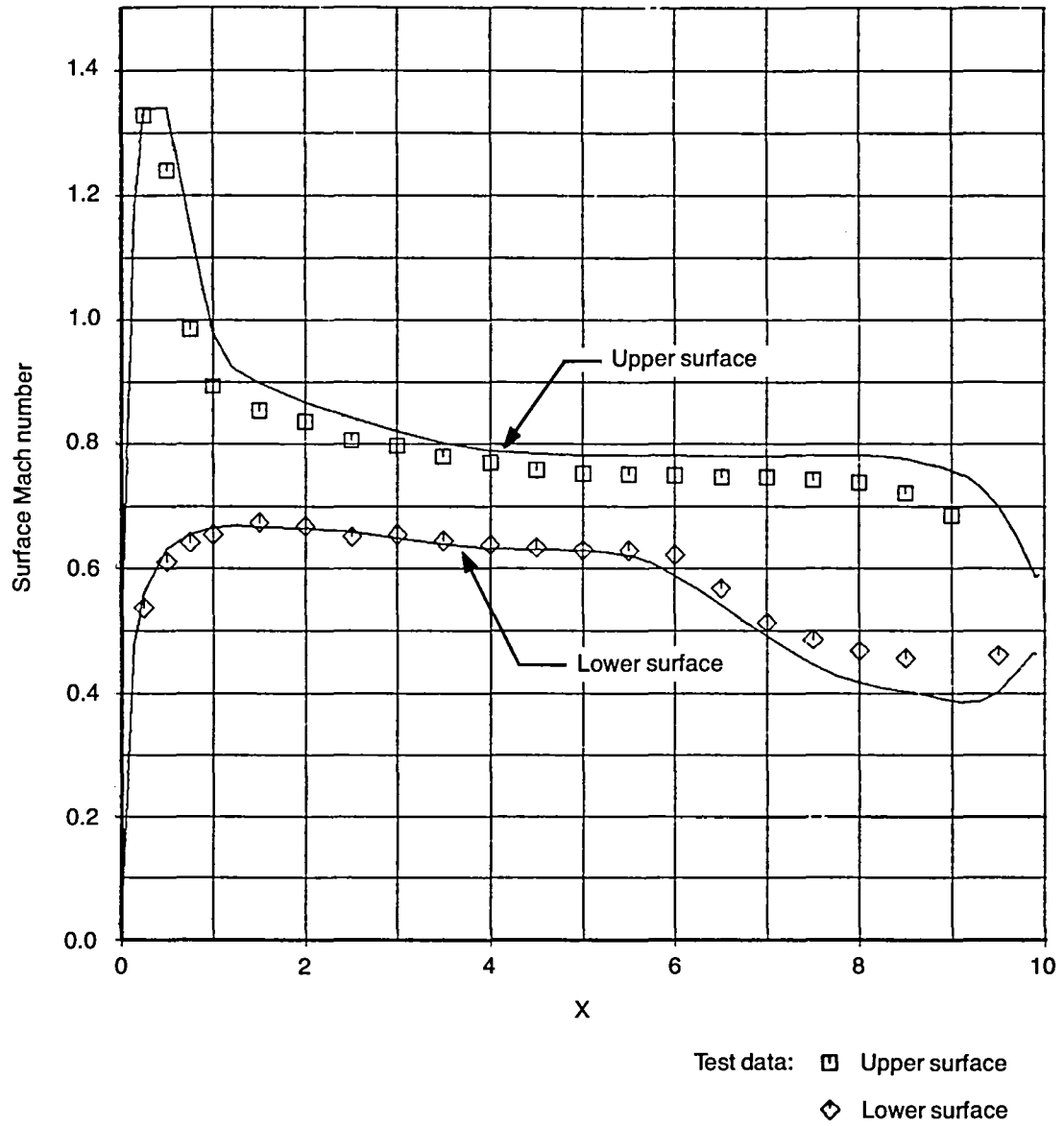
Figure 8. NASA Wing, Pylon, and Nacelle Model,  $M_\infty = 0.2$ , Angle of Attack = 5.0 deg, Configuration 5,  $D = 4.5$  in



Test data:  $\diamond$  90.0°  
 $\circ$  180.0°  
 $\triangle$  270.0°

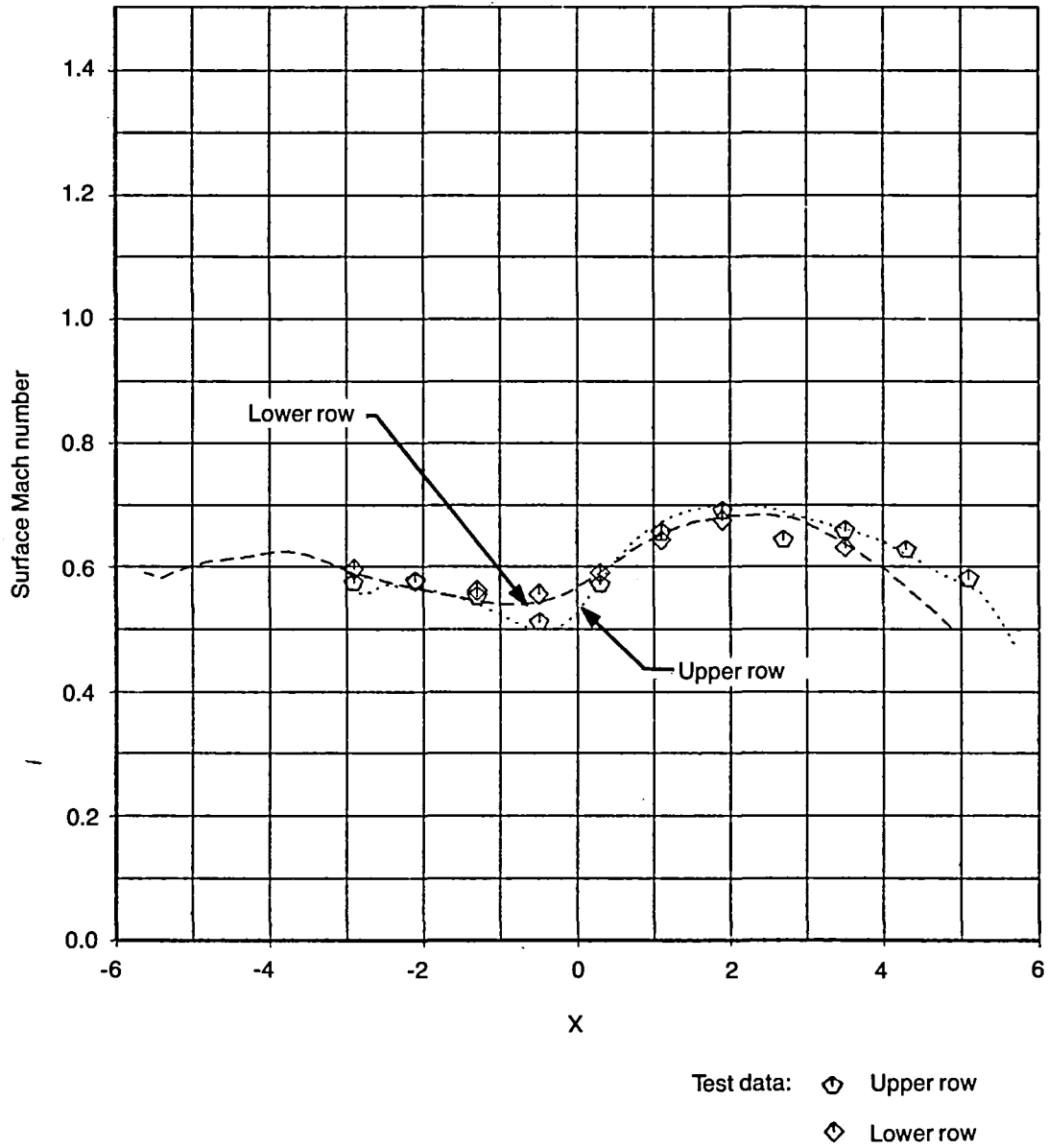
(c) Nacelle Surface Mach Number

Figure 8. NASA Wing, Pylon, and Nacelle Model,  $M_\infty = 0.2$ , Angle of Attack = 5.0 deg, Configuration 5,  $D = 4.5$  in



(a) Wing Surface Mach Number,  $y/D = 0.5$

Figure 9. NASA Wing, Pylon, and Nacelle Model,  $M_\infty = 0.6$ , Angle of Attack = 3.0 deg, Configuration 5,  $D = 4.5$  in



(b) Pylon Surface Mach Number

Figure 9. NASA Wing, Pylon, and Nacelle Model,  $M_\infty = 0.6$ , Angle of Attack = 3.0 deg, Configuration 5,  $D = 4.5$  in

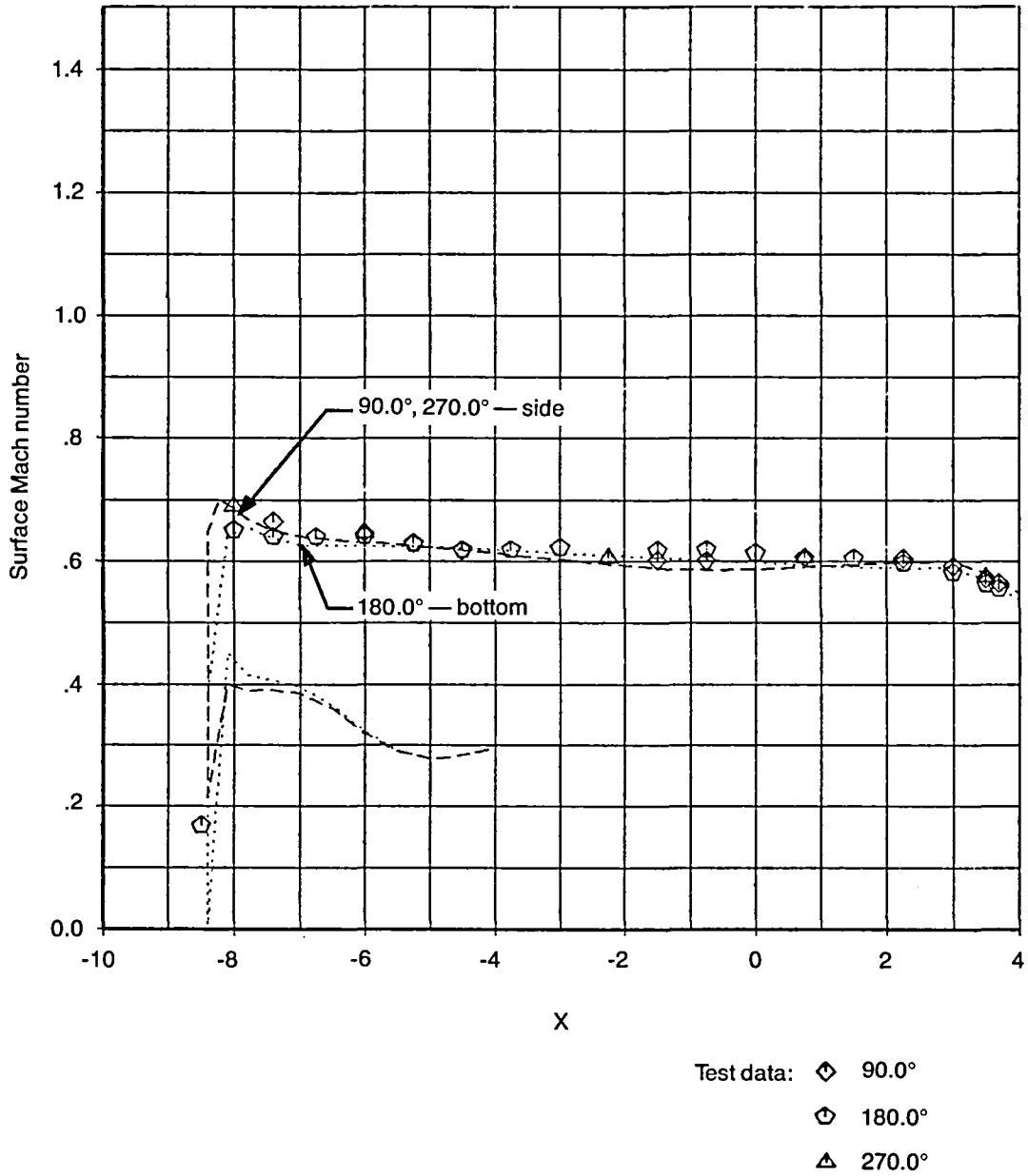
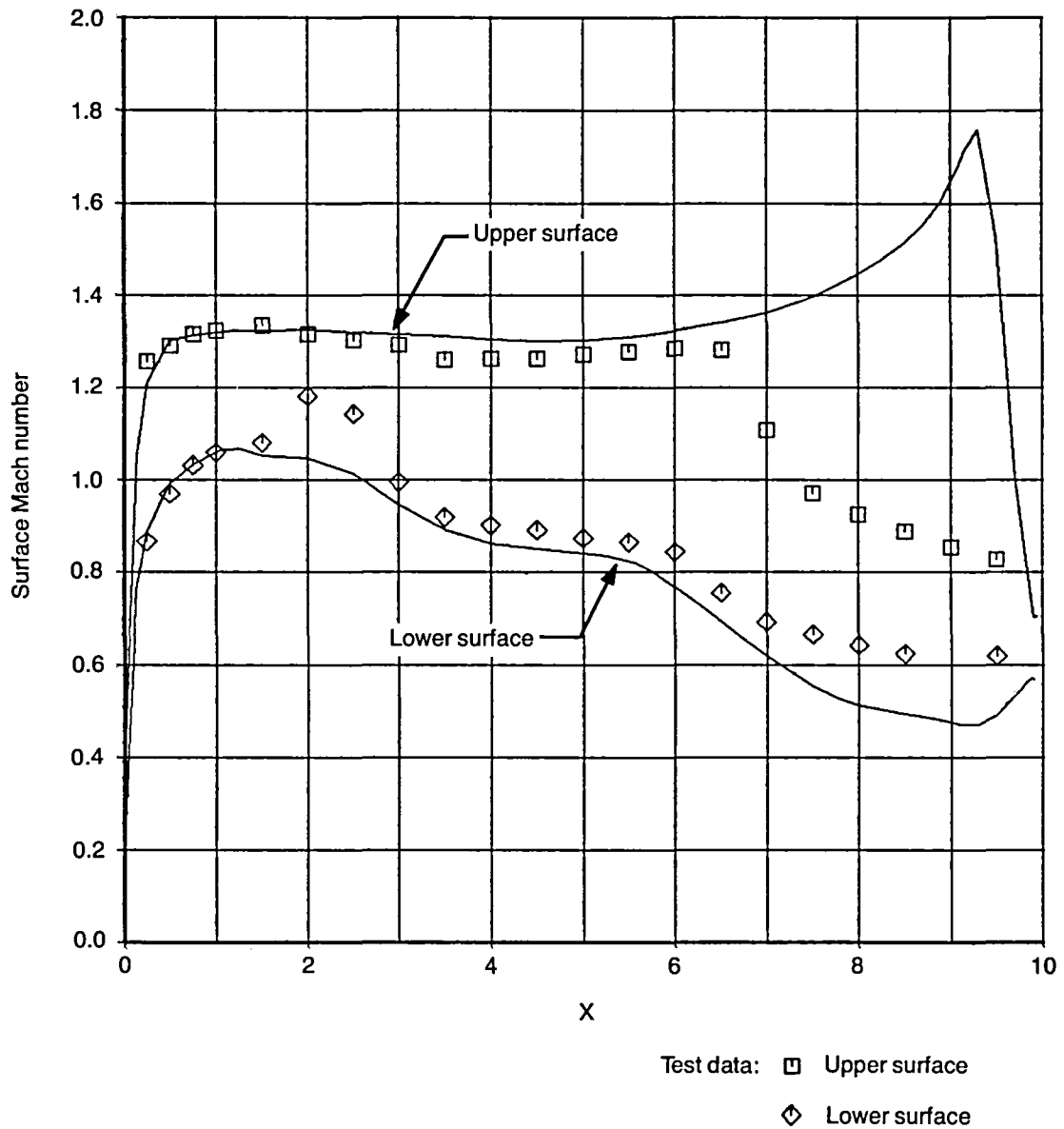


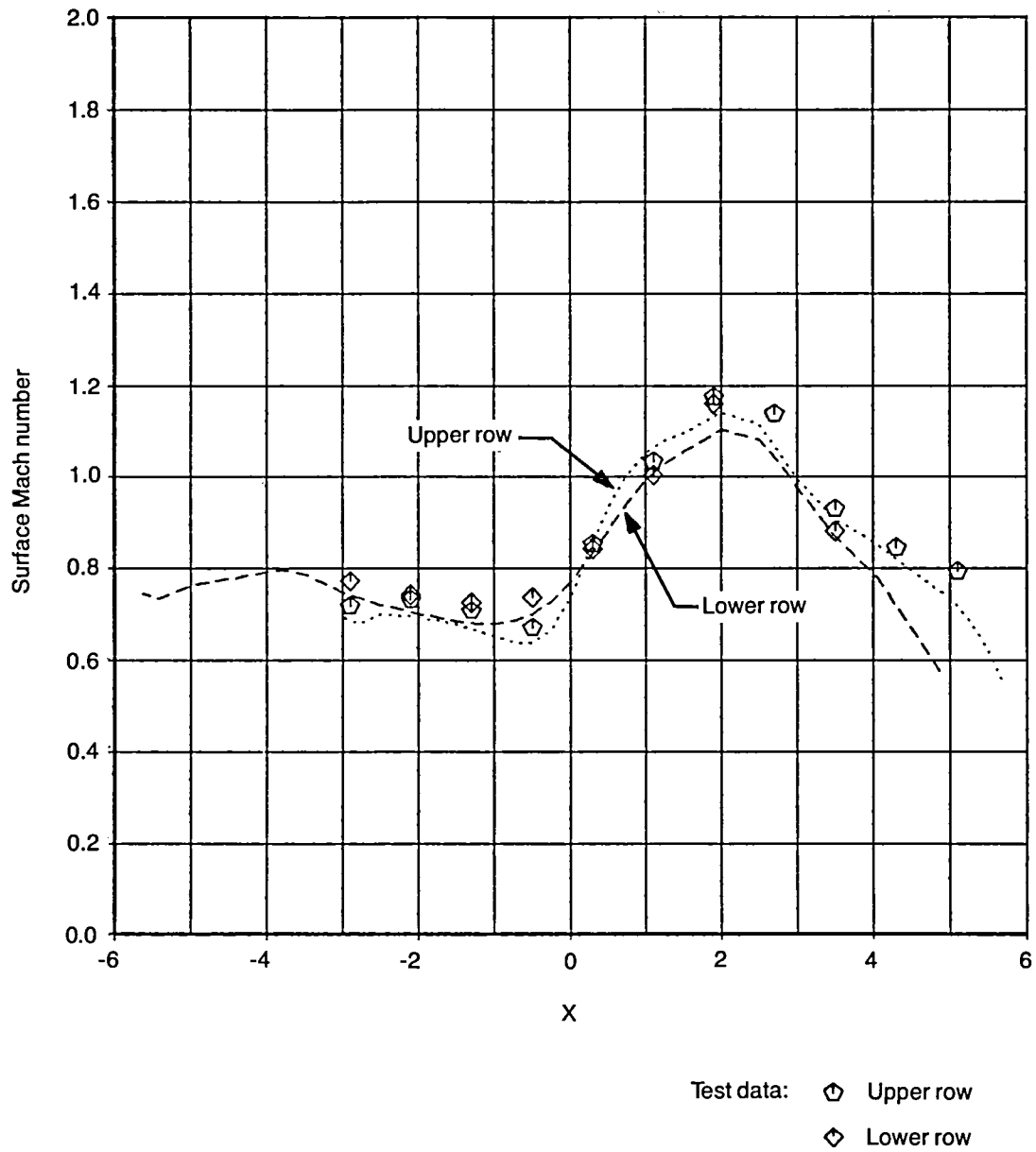
Figure 9. NASA Wing, Pylon, and Nacelle Model,  $M_\infty = 0.6$ , Angle of Attack = 3.0 deg, Configuration 5,  $D = 4.5$  in





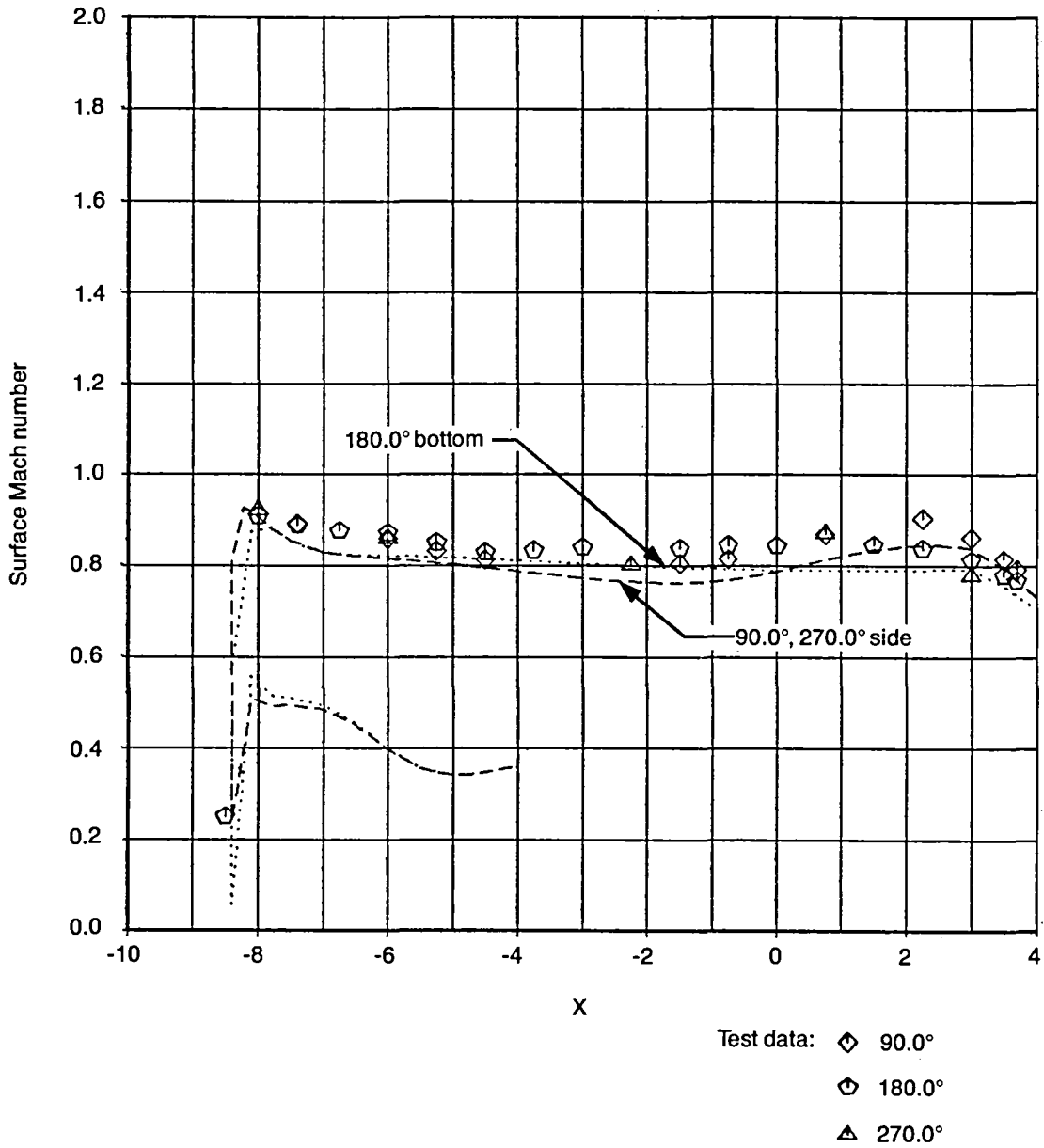
(a) Wing Surface Mach Number,  $y/D = 0.5$

Figure 10. NASA Wing, Pylon, and Nacelle Model,  $M_\infty = 0.8$ , Angle of Attack = 2.0 deg, Configuration 5,  $D = 4.5$  in



(b) Pylon Surface Mach Number

Figure 10. NASA Wing, Pylon, and Nacelle Model,  $M_\infty = 0.8$ , Angle of Attack = 2.0 deg, Configuration 5,  $D = 4.5$  in



(c) Nacelle Surface Mach Number

Figure 10. NASA Wing, Pylon, and Nacelle Model,  $M_\infty = 0.8$ , Angle of Attack = 2.0 deg, Configuration 5,  $D = 4.5$  in

## 5.0 USE OF THE PROGRAM

This section describes part of the procedure for using the computer program based on the analysis described in the last section. Those subjects not discussed are control cards and preparation of the geometry. Mesh selection is discussed. Samples of input and output files are presented. Some guides to possible failure modes are provided.

The process of specifying a three-dimensional geometry and intersecting it with a mesh is a major task by itself. Therefore this procedure is documented separately (ref. 7). The computer program has been designed so that the geometry information can come from any source. The file of surface-mesh intersects, coordinates, and normals does not have to have any special ordering. The geometry documents previously referred to are guides to one possible way to generate the geometry portion of the input file, but certainly not the only way.

The control cards for executing the code on the computer are not described in this document. Operating systems, field lengths, file names, etc. change relatively frequently so it is not advisable to document procedures that will probably be different by the time the document is read.

The analysis currently exists in versions for both the CDC CYBER 203 computer and the CRAY-1 computer. This report describes the latest version of the program encompassing the capabilities of the earlier versions of the computer code.

### 5.1 INPUT FORMAT

The first two lines of the input file are title lines and are printed at the start of the output for identification purposes. All input except for the title lines is by means of *order independent* groups headed by key words. The purposes of this particular input format are to allow certain groups to be optional, make the input file more readable, facilitate checking of input data by the program, and make future additions to the program easier. Certain input groups are mandatory, while others are optional and may be omitted. All input, except for title lines and comment lines, consists of numbers or words (depending on group) in fields of 10 columns wide, *maximum of six fields per input line*. All numbers are *floating point* and require a decimal point. Only the first four characters of key words are checked.

Certain interrelations among various input groups have to be taken into account. If convergence is to be obtained on a sequence of meshes, the *number* of x, y, and z, or x, r, and  $\theta$  mesh can only have certain values. This is because coarser meshes are formed by deleting every other mesh line. Also, a compressor face, if there is one, must lie on an x mesh belonging to the coarsest mesh. There are restrictions on the number of mesh and number of surface points relating to declared array lengths in the computer code. These limits as they currently exist are listed in Section 5.1.3.

The program has the capability to use up to four mesh-density levels to provide more efficient convergence. The number of levels is controlled by the SWEEPS option. The mesh and geometry for the finest mesh level must be input. Coarser meshes for x, y, z, and r are formed by deleting *exactly* every other mesh from the previous mesh. This places restrictions on the number of mesh allowed in the finest mesh, as the first and last mesh line have to remain when every other mesh is deleted. The  $\theta$  mesh is a special case. There is an option to control the manner in which the  $\theta$  mesh is varied between levels. The number of  $\theta$  mesh can be held constant for two successive levels, or every other  $\theta$  mesh value can be deleted for the coarser mesh.

The program allows the use of planes of symmetry for *cylindrical coordinates* to reduce the number of mesh needed to make a calculation. For a cylindrical mesh, if the largest  $\theta$  mesh value input is 180.00 deg, the plane 0= 0 deg, and 180 deg is taken to be a plane of symmetry. If the largest  $\theta$  mesh input is less than 180 deg, the flow is assumed symmetrical about 0 deg and the largest  $\theta$  value input. Zero deg must always be input as a theta mesh.

### 5.1.1 SUMMARY OF INPUT GROUPS

#### REQUIRED

Keyword	Description
	Title lines
FREEstream	Speed of sound, freestream velocity and flow angles
XMESH	Axial mesh values
YMESH	} or y or radial mesh values
RMESH	
ZMESH	} or z or circumferential mesh values
TMESH	
GEOMETRY	Surface-mesh intersections: coordinate and surface normal values

#### OPTIONAL

Keyword	Description
COMMENT	Allows comments describing the run to be printed on the first page of the output
WING	Indicates lifting surface calculation
CFACE	Indicates an inlet geometry and specifies inlet mass flow and location of the compressor face
SWEEps	Convergence control parameters
COPT	Allows changing the criteria for the multigrid cycling between meshes
ADI	Controls type of lines, y or z, r or $\theta$ , used for line relaxation. Allows requesting alternating y and z (r and $\theta$ ) lines
THETA	Control of number of $\theta$ planes for each mesh-density level (cylindrical coordinates only)
SCDiff	Indicates special $\theta$ differencing to be used (cylindrical coordinates only)
PRINT op	Requests printout of various categories of geometric information
SFLOW	Requests surface flow variable printout at end of run
OUTT	Allows surface quantities to be printed in an alternate coordinate system
FLDT	Requests printout of flow variables at constant z or $\theta$ cuts of flowfield
IPRI	Requests printout at other than level 4 for multilevel calculation
NOMG	Suppresses multigrid convergence procedure
PLOT	Surface quantities are written to file FT03 in a format for IGDA GGP plots (BCS CRAY-1 version) only
RELX	Allows the specification of the over- or under-relaxation factors

## OPTIONAL (Diagnostic)

Keyword	Description
DEBUg	Requests print of coefficients, velocities, and potential function for a specified axial cut and sweep number

### 5.1.2 DETAILED INPUT-GROUP DESCRIPTIONS

#### FREESTREAM

This group specifies the velocity and orientation for the freestream relative to the geometry.

The scaling of the velocities is essentially arbitrary except that they should be of order one to avoid difficulties with print formats. Note that  $q_\infty/a_\infty = M_\infty$ .

Required input group, no default values.

Card 1	Cols.	1-4	'FREE', Keyword
Card 2	Cols.	1-10	$a_\infty$ , freestream speed of sound
		11-20	$q_\infty$ , freestream velocity
		21-30	$\alpha_1$ , degrees, $\arctan(v_\infty/u_\infty)$
		31-40	$\alpha_2$ , degrees, $\arctan(w_\infty/u_\infty)$

Special conventions:

If  $\alpha_1 = 90$  deg,  $\alpha_2 = \arctan(w_\infty/v_\infty)$  ( $u_\infty = 0.0$ ).

If  $\alpha_1 = 90$  deg and  $\alpha_2 = 90$  deg,  $w_\infty = q_\infty$  ( $u_\infty = v_\infty = 0.0$ ).

If airplane coordinates are used (z oriented up),  $\alpha_2$  is the angle of attack and  $\alpha_1$  is a yaw angle.

If cylindrical coordinates are used with  $\theta = 0$  deg as the top or crown (inlet calculation),  $\alpha_1$  is the angle of attack and  $\alpha_2$  is a yaw angle.

Note: Input of "FREE STREAM" which is 11 characters instead of "FREE" or "FREESTREAM" will draw an error message.

#### XMESH

YMESH or RMESH

ZMESH or TMESH

These groups handle the input of the computational mesh, x, y, and z or x, r, and theta, theta in degrees. The values do not have to be in any order. Theta mesh must include 0, 90, 180, and 270 deg unless there is a plane of symmetry. Zero deg must always be included as a theta mesh.

The program creates lower mesh levels by deleting every other mesh value from the previous mesh. Also, the first and last mesh must remain and the compressor face, if there is one, must be in the coarsest mesh. If L is the number of mesh levels (see SWEEPS Group), then NX and NY (NR) can have the following values:

$$L = 4 \quad NX \text{ or } NY = 25, 33, 41, \dots, (8m+1) \quad (m \text{ an integer})$$

$$L = 3 \quad NX \text{ or } NY = 13, 17, 21, \dots, (4m+1)$$

The number of z mesh behaves the same. For cylindrical coordinates, similar rules apply, except it is possible to keep the number of  $\theta$  mesh constant for two adjacent levels and a periodic mesh (0 to 360 deg) is possible. See the THET option for the rules for such meshes.

See Section 5.2 for a discussion of the number of levels that can or should be used.

Required input groups, no default values.

Card 1	Cols.	1-4 11-20	'_MES', Keyword, _ can be X, Y, and Z or X, R, and T (theta) Number of mesh values to be read
Card 2	Cols.	1-10 11-20 21-30 : :	} Axial, y or radial, or z or circumferential location of mesh, six values per card, as many cards as required. Theta must be in degrees.

See Section 5.1.3 for the maximum number of mesh that can be used.

### GEOMETRY

This group consists of the coordinates of the intersections of the mesh with the geometry and the direction cosines of the surface normal at each intersect.

Required input group, no default values.

Card 1	Cols.	1-4 11-20	'GEOM', Keyword number of intersects, NSURTOT
Card 2	Cols.	1-10 11-20 21-30 31-40 41-50 51-60	} one intersect per card
		x y or r z or $\theta$ (degrees) $n_x$ $n_y$ or $n_r$ $n_z$ or $n_\theta$	
Card 3	Cols.	1-10 : :	
Card			
NSURTOT+1			

Note:

- (1) See Section 5.1.3 for maximum value of NSURTOT.
- (2) Surface normal is unit surface normal ( $n_x^2+n_y^2+n_z^2=1.0$ ) and must be oriented into the flowfield.

COMMENT (Optional)

This group allows a multiline comment to be printed on the first page of a computation. This allows a longer description of a run than can be achieved using the required two title cards.

Card 1	Cols.	1-4 11-20	'COMM', Keyword Number of comment cards to be read
Card 2	Cols.	1-80	1st comment card
Card 3	Cols.	1-80	2nd comment card
.	.	.	.
.	.	.	.

WING (Optional)

This option allows lifting surface calculations, that is, wings with a Kutta boundary condition applied at the trailing edge. The program automatically locates wing-like surfaces.

Card 1	Cols.	1-4	'WING', Keyword
--------	-------	-----	-----------------

CFACE (Optional)

Signals that there is an inlet geometry and specifies the Mach number and station (x) of the compressor face.

Card 1	Cols.	1-4	'CFAC', keyword
Card 2	Cols.	1-10 11-20	x value at compressor face Mach number to be enforced at compressor face

The x station specified must be consistent with the input geometry and must be a mesh value for the coarsest mesh. The Mach number specified is the one-dimensional flow average Mach number for a cylinder with the cross-sectional area of the compressor face.

SWEEPS (Optional)

This group controls the sweeping process by allowing control of the number of mesh-density levels, the maximum number of sweeps on each mesh-density level, and a convergence criterion for each mesh-density level. The mesh numbering system is such that level 4 is the finest mesh. Levels 3, 2, and 1 may or may not exist. The number of levels to be used is set by the number of values entered for maximum number of sweeps on a level. There will be as many levels used as nonzero values entered.



In general, it is difficult to determine in advance how many mesh levels to use in a calculation. The multigrid is theoretically most efficient with many levels, but if the mesh becomes quite coarse relative to the geometry, the program can behave badly or fail on the coarser mesh levels. For standard calculations (not more than 56 000 grid points), three levels is probably the maximum that should be used. Less than three levels can be tried if the program fails while trying to use three levels.

Default is a three-level mesh with the following limits:

Level	2	3	4
Maximum number of sweeps	800.0	200.0	100.0
Convergence parameter	1.0	1.0	1.0

Card 1 Cols. 1-4 "SWEE", Keyword.

Card 2 Cols. 1-10 } Maximum number of sweeps allowed at each level.  
 11-20 } Coarsest mesh limit first and finest mesh limit last.  
 21-30 } One to four values. This card sets the number of  
 31-40 } levels to be used in the calculation.

Card 3 Cols. 1-10 } Convergence parameters for each level, coarsest level  
 11-20 } limit first, finest level limit last. Sweeping on a  
 21-30 } level is stopped and convergence is assumed  
 31-40 } when the average value of  $|\Delta\phi|$  (change in  $\phi$  between sweeps) multiplied by  $10^6$  and divided by  $(\phi_{\max} - \phi_{\min})$  is less than the value of the convergence parameter for that level.

Example:

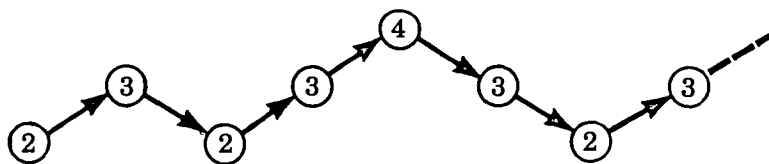
Two-level calculation, maximum of 500 sweeps for the coarsest level, level 3, and 100 sweeps for the finest level. The calculation to be converged to a relative error of  $0.5 \times 10^{-6}$  on level 3 and  $10^{-6}$  on level 4.

```
SWEE
500.0  100.0
0.5    1.0
```

COPT (Optional)

This option allows control of the convergence procedure used. The options are adaptive cycling, fixed cycling with default limits, or fixed cycling with user specified limits. The adaptive cycling does not move to a higher (denser) level until convergence is reached at the current level. This can cause a run failure if it happens that the calculation is unstable at one of the intermediate levels. The default for this option is fixed cycling with default limits. It is recommended that the adaptive cycling option not be used. The default method, in general, is the most reliable convergence option.

The default cycling pattern for a three-level calculation is diagrammed below:



where  $\textcircled{n}$  indicates sweeping on level n.

Level 2 is swept until convergence or 100 sweeps have been taken. Levels 3 and 4 are swept a minimum of six sweeps and a maximum of 20 sweeps. Sweeping on levels 3 and 4 is stopped if convergence or stalling occurs. Level 4 is visited at least twice and a maximum of 4 times.

Card 1	Cols.	1-4	"COPT", Keyword
		11-20	0.0 adaptive cycling
			1.0 fixed cycling with default limits on the number of sweeps per visit to a level and the number of visits to any level (default)
			2.0 fixed cycling with limits input

If the COPT option equals 2.0, the following cards are required:

Card 2	Cols.	1-10	} Floating point values for the maximum number of sweeps per visit on each level starting with the lowest (coarsest) mesh level and ending with level 4. 1st value in cols. 1-10. One to four values depending on number of levels to be used (see "SWEE" option).
		11-20	
		21-30	
		31-40	

Card 3	Cols.	1-10	} Floating point values for maximum number of visits to each level ordered as above.
		11-20	
		21-30	
		31-40	

Default values (COPT option equals 1.0)

100 sweeps maximum per visit on the lowest level (coarsest mesh)

20 sweeps maximum per visit otherwise

4 = maximum number of visits to finest level

Example:

Three level calculation, default limits input explicitly.

COPT	2.0	
100.0	20.0	20.0
20.0	20.0	4.0

ADI (Optional)

This option permits user control over the direction of the lines for line relaxation. Either y (r) or z ( $\theta$ ) lines may be used or y and z lines can be used alternately.

Default is z lines for Cartesian meshes and r (radial) lines for cylindrical coordinates.

Card 1	Cols.	1-3	'ADI', Keyword
		4	Blank
		11-20	1.0 = y or r (radial) lines used
			2.0 = z or $\theta$ lines used
			3.0 = alternate y and z or r and $\theta$ lines starting with y (r) lines

THETA (Optional)

This group allows control of the number of  $\theta$  grid used for each mesh-density level (cylindrical coordinate calculation only). The number of levels used is controlled by the SWEEPS option (default is four levels), and this option must be consistent with the SWEEPS option input. The

number of  $\theta$  grid at level  $i$ ,  $NT_i$ , may be held the same as level  $i+1$  or every other grid of level  $i+1$  can be deleted to form level  $i$ . The value specified for the number of  $\theta$  grid at the finest level must be the same as used in the TMESH input group, and the values specified for coarser levels must be consistent with any flow symmetry that has been specified (TMESH input group).

Default for this option is no change in the number of  $\theta$  mesh used for different levels.

Card 1	Cols.	1-4	'THET', Keyword
Card 2	Cols.	1-10 11-20 21-30 31-40	} Number of $\theta$ grid for each level, coarsest level first and finest level last, one to four values starting in cols. 1-10

Notes:

(1) If there is a plane of symmetry (less than 0-deg to 360-deg geometry input)

$$NT_i = NT_{i+1} \text{ or } NT_i = (NT_{i+1} + 1) / 2.0,$$

otherwise,

$$NT_i = NT_{i+1} \text{ or } NT_i = NT_{i+1} / 2.0.$$

SCDIFF (Optional)

This group allows use of special  $\theta$  differencing (ref. 1) for improved accuracy with very coarse  $\theta$  meshes (cylindrical coordinate calculations).

Default is regular differencing.

Card 1	Cols.	1-4 11-20	'SCDI', Keyword 0.0 regular differencing 1.0 special $\theta$ differencing (any other value than 0.0 or 1.0 will be treated as 0.0)
--------	-------	--------------	---

PRINT OP (Optional)

Inputs any or all of a group of keywords to obtain printed output of a variety of geometrical information.

Card 1	Cols.	1-4	'PRIN', Keyword
Card 2	Cols.	1-10 11-20 . . .	} Up to five keywords as described below. Can be in any order (only first four characters of keyword are checked).

<u>SPINPUT</u>	List of the surface points in the order read.
<u>SPORDER</u>	List of surface points in the internal ordering used in the analysis.
<u>SPECPTS</u>	List of special points.

<u>TYPE2</u>	List of Type 2 points. These are points that are both surface and mesh nodes.
<u>MAP</u>	Lists of x, y, and z, or x, r, and $\theta$ constant cuts of the surface. Lists include surface-point indexes, surface-point coordinates, arc length along the cuts, and components of the surface normals.

The default is none of the above output.

SFLOW (Optional)

This group controls printing of flow properties along the surface. Default is printing of every fourth cut for all surfaces. This default corresponds to coarse-mesh cuts for a three-level calculation.

Card 1	Cols.	1-4	'SFLO', Keyword
Card 2	Cols.	1-10	SKIPX value
		11-20	SKIPR value
		21-30	SKIPT value

For the fine mesh, every constant x cut will be printed if SKIPX = 1. If SKIPX = 0, no cuts will be printed. Otherwise, cuts will be printed for  $x = X(I), I = 1, 1 + \text{SKIPX}, 1 + 2*\text{SKIPX}, \text{etc.}$  SKIPR and SKIPT work the same for y or r, and z or  $\theta$  constant cuts of the surfaces, respectively.

OUTT (Optional)

It is often desirable or necessary to use more than one coordinate system. As an example, an inlet may be described by either an engine centerline or an inlet centerline coordinate system, and the user may alternate between the two depending on the situation. This option allows output of flow properties along the surface in a coordinate system different from that of the computation.

Card 1	Cols.	1-4	'OUTT', Keyword (output transformation)
		11-20	1.0 transformed coordinate output only
			2.0 regular output <i>and</i> transformed coordinate output
Card 2	Cols.	1-10	0.0 transformed coordinates are Cartesian
			1.0 transformed coordinates are cylindrical
		11-20	} Same as SFLO option } except apply to transformed } coordinate output only
		21-30	
		31-40	
Card 3	Cols.	1-10	$\Delta x_1$
		11-20	$\Delta y_1$
		21-30	$\Delta z_1$
		31-40	$\Delta x_3$
		41-50	$\Delta y_3$
		51-60	$\Delta z_3$
Card 4	Cols.	1-10	$t_{11}$
		11-20	$t_{12}$
		21-30	$t_{13}$

Card 5 Cols. 1-10  $t_{21}$   
 11-20  $t_{22}$   
 21-30  $t_{23}$

Card 6 Cols. 1-10  $t_{31}$   
 11-20  $t_{32}$   
 21-30  $t_{33}$

The transformation is defined as follows where the subscript 1 indicates the initial coordinates and the subscript 4 the final coordinates:

Note  $(t_{ij})$  must be such that :

$$\begin{bmatrix} t_{11} & t_{12} & t_{13} \\ t_{21} & t_{22} & t_{23} \\ t_{31} & t_{32} & t_{33} \end{bmatrix} \times \begin{bmatrix} t_{11} & t_{21} & t_{31} \\ t_{12} & t_{22} & t_{32} \\ t_{13} & t_{23} & t_{33} \end{bmatrix} = \begin{bmatrix} 1.0 & 0.0 & 0.0 \\ 0.0 & 1.0 & 0.0 \\ 0.0 & 0.0 & 1.0 \end{bmatrix}$$

i.e.,

$$\sum_{k=1}^3 t_{ik}t_{jk} = \delta_{ij} \quad \begin{matrix} \delta_{ij} = 1 & i = j \\ \delta_{ij} = 0 & i \neq j \end{matrix}$$

$$\left. \begin{matrix} y_1 = r_1 \cos\theta_1 \\ z_1 = r_1 \sin\theta_1 \end{matrix} \right\} \quad \begin{matrix} \text{if initial coordinates} \\ \text{are cylindrical,} \end{matrix}$$

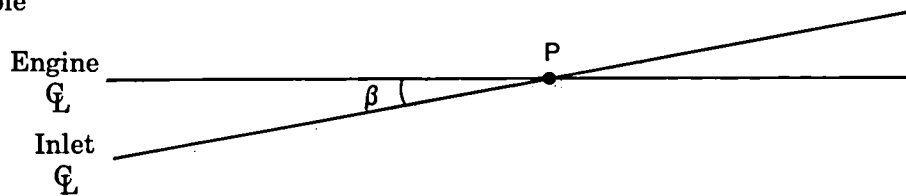
$$\begin{matrix} x_2 = x_1 + \Delta x_1 \\ y_2 = y_1 + \Delta y_1 \\ z_2 = z_1 + \Delta z_1 \end{matrix}$$

$$\begin{bmatrix} x_3 \\ y_3 \\ z_3 \end{bmatrix} = \begin{bmatrix} t_{11} & t_{12} & t_{13} \\ t_{21} & t_{22} & t_{23} \\ t_{31} & t_{32} & t_{33} \end{bmatrix} \begin{bmatrix} x_2 \\ y_2 \\ z_2 \end{bmatrix}$$

$$\begin{matrix} x_4 = x_3 + \Delta x_3 \\ y_4 = y_3 + \Delta y_3 \\ z_4 = z_3 + \Delta z_3 \end{matrix}$$

$$\left. \begin{matrix} r_4 = \sqrt{y_4^2 + z_4^2} \\ \theta_4 = \arctan(y_4/z_4) \end{matrix} \right\} \quad \text{if final coordinates are cylindrical.}$$

Example



Note that y is the vertical coordinate and z the side coordinate for this example.

If in engine centerline coordinates point P has coordinates:

$$\begin{matrix} x = a \\ r = 0.0 \\ \theta = - \end{matrix}$$

and in inlet centerline coordinates point P has coordinates:

$$\begin{aligned}x &= b \\r &= 0.0 \\ \theta &= -,\end{aligned}$$

then for calculation in engine centerline coordinates - print in inlet centerline coordinates,

$$\begin{aligned}\Delta x_1 &= -a \\ \Delta y_1 &= 0.0 \\ \Delta z_1 &= 0.0 \\ \Delta x_3 &= b \\ \Delta y_3 &= 0.0 \\ \Delta z_3 &= 0.0 \\ t_{11} &= \cos\beta \\ t_{12} &= \sin\beta \\ t_{13} &= 0.0 \\ t_{21} &= -\sin\beta \\ t_{22} &= \cos\beta \\ t_{23} &= 0.0 \\ t_{31} &= 0.0 \\ t_{32} &= 0.0 \\ t_{33} &= 1.0.\end{aligned}$$

For calculation in inlet centerline coordinates - print in engine centerline coordinates,

$$\begin{aligned}\Delta x_1 &= -b \\ \Delta y_1 &= 0.0 \\ \Delta z_1 &= 0.0 \\ \Delta x_3 &= a \\ \Delta y_3 &= 0.0 \\ \Delta z_3 &= 0.0 \\ t_{11} &= \cos\beta \\ t_{12} &= -\sin\beta \\ t_{13} &= 0.0 \\ t_{21} &= \sin\beta \\ t_{22} &= \cos\beta \\ t_{23} &= 0.0 \\ t_{31} &= 0.0 \\ t_{32} &= 0.0 \\ t_{33} &= 1.0.\end{aligned}$$

### FLDT (Optional)

This option determines z or  $\theta$  mesh values for which the field properties are to be printed. Default is no field printout.

Card 1	Cols.	1-4 11-20	'FLDT', Keyword. NFFPR, number of z or $\theta$ values for which field properties are to be printed. NFFPR = 0.0 or NFFPR < 0.0 has special significance as described.
--------	-------	--------------	---

If  $NFFPR = 0.0$ , the entire flowfield is printed. Warning - this can cause an excessive quantity of printout.

If  $NFFPR > 0.0$ , the following cards are required:

Card 2	Cols.	1-10	} Values of z or $\theta$ mesh for printing field properties, 6 values per card ( $\theta$ in degrees)
		11-20	
		.	
.	.	.	
.	.	.	
.	.	.	

If  $NFFPR < 0.0$ , the flowfield is printed between specified x values for each z or  $\theta$  constant plane requested. The following cards are required:

Card 2	Cols.	1-10	T1	Field is printed for the z or $\theta$ mesh value(s), TI for $XI1 \leq x \leq XI2$
		11-20	X11	
		21-30	X12	

Card 3	Cols.	1-10	T2
		.	X21
		.	X22
.	.	.	.

Card |NFFPR|  
+1

#### IPRI (Optional)

This option allows printing of solution properties for the coarse meshes including mass-flow conservation computation. Default is no solution printout for coarse meshes. Printout occurs only if convergence is obtained. The 0.0 option for the COPT group works best with this option.

Card 1	Cols.	1-4	'IPRI', Keyword
--------	-------	-----	-----------------

#### NOMG (Optional)

This keyword causes the program to use a multilevel procedure instead of the more efficient multigrid convergence procedure. The multilevel procedure is defined as a calculation on a sequence of successively finer grids. A multigrid calculation is a cycling between grids using coarse grid calculations to obtain corrections to the fine grid solution. *Use of this option is not recommended.*

Card 1	Cols.	1-4	'NOMG', Keyword
--------	-------	-----	-----------------

#### PLOT (Optional) - CRAY-1 version only

This option allows surface flow properties to be written to disk in a format suitable for plotting using the GGP plotting program on the Boeing IGDA graphics computer systems.

Card 1	Cols.	1-4 11-20	'PLOT', Keyword Number of constant coordinate curve families to be saved. These can be x constant cuts, y or r constant cuts, or z or $\theta$ constant cuts of the surface. Limit is 3.0.
Card 2	Cols.	1-10 11-20 21-30	} One to three values depending on number of curve families requested. 1.0 to save x-constant cut information, 2.0 to save y- or r-constant information, 3.0 to save z- or $\theta$ -constant information.

Examples:

PLOT	2.0		} To save x- and z ( $\theta$ )-constant cuts
1.0	3.0		
PLOT	3.0		} To save everything
1.0	2.0	3.0	

Note: Plot information is written to disk (file FT03) and control cards are required to save the disk file.

### RELX (Optional)

This option allows the user to specify the over- or under-relaxation factors used in the code. Use of this option is not recommended. If multigrid is being used, the over-relaxation factors are used only for the coarsest grid. Under-relaxation factors are used for all grids.

Default values are  $\omega_x = 1.85$ ,  $\omega_y$  ( $\omega_r$ ) = 0.90, and  $\omega_z$  ( $\omega_\theta$ ) = 0.90.

Card 1	Cols.	1-4	'RELX', Keyword
Card 2	Cols.	1-10	$\omega_x$
		11-20	$\omega_y$ ( $\omega_r$ )
		21-30	$\omega_z$ ( $\omega_\theta$ )

Note:  $0 < \omega < 2.0$  required for stable solution.

### DEBUG (Optional)

Diagnostic print option. Prints internal parameters for a given x mesh index and sweep number.

Card 1	Cols.	1-4	'DEBU', Keyword
Card 2	Cols.	1-10	Sweep number
		11-20	x-plane index

### 5.1.3 Limits and Timing

The limits on the number of mesh and the number of surface points are due to the declared array lengths in the code. They are subject to change. Current limits are given on Table 1. These limits are set with respect to the computer memory available, but could be increased to some extent.



Table 1. Program Internal Limitations

NX	161
NY (NR)	121
NZ (NT)	121 *
NX*NY	8 500
NX*NZ	8 500
NY*NZ	4 250
NX*NY*NZ	252 105
Number of surface points	8 500
Number of surface points on or adjacent to any x constant plane	500
Number of surface points on or adjacent to any z ( $\theta$ ) constant plane	1 000
Maximum number of planes of field print out (NFFPR for FLDT input group)	200

\*120 for a periodic mesh (i.e., 0 to 360 deg)

The CRAY-1 version of the code presently requires approximately 1 600 000 words of memory. A maximum case on the NASA Langley Research Center CDC C-203 computer (a virtual memory machine with 1 million word real memory, but soon to be increased) will be very expensive (with the 1 million word real memory) because of the page faults. It is best to run smaller cases on this machine until the memory is increased.

Typical run times on the CRAY-1 are 1 to 2 min for 50 000 field points and 3 to 5 min for 250 000 field points. Run times on the CDC C-203 computer are approximately twice as long.

#### 5.1.4 Sample Inputs

The first page of the listings of three different data cases are presented as examples (figs. 11, 12, 13). These files have been arranged so that the geometry group, by far the longest, is last. This is not required, but does make the files much easier to work with.

```

QFAN INLET REF. NASA CR151922, SYBERG, J. AND KONCSEK, J. D. v JAN. 1977
MACH INF. = 0.21 ALPHA = 60.0 DEGREES P465 DEMONSTRATION TEST CASE
FREESTREAM
1.0 0.21 60.0 0.0
SWEEPS
800. 200. 100.
1. 1. 1.
SFLOWPR
1.0 1.0 1.0
IPRI
THET
9.0 9.0 9.0
CFACE
45.012 0.43
X MESH 69.
-180.0480 -168.7950 -157.5420 -146.2890 -135.0360 -123.7830
-112.5300 -101.2770 -90.0240 -83.2722 -76.5204 -69.7686
-63.0168 -56.2650 -49.5132 -42.7614 -36.0096 -31.5084
-27.0072 -22.5060 -18.0048 -15.7542 -13.5036 -11.2530
-9.0024 -7.8771 -6.7518 -5.6265 -4.5012 -3.3872
-2.2731 -1.1591 -.0450 1.0915 2.2281 3.3646
4.5012 5.6265 6.7518 7.8771 9.0024 11.2530
13.5036 15.7542 18.0048 20.2554 22.5060 24.7566
27.0072 29.2578 31.5084 33.7590 36.0096 38.2602
40.5108 42.7614 45.0120 47.2626 49.5132 51.7638
54.0144 58.5156 63.0168 67.5180 72.0192 76.5204
81.0216 85.5228 90.0240
R MESH 49.
0.0000 1.4450 2.8900 4.3350 5.7800 7.2250
8.6700 10.1150 11.5600 13.0050 14.4500 15.8950
17.3400 18.7850 20.2300 21.6750 23.1200 23.8425
24.5650 25.2875 26.0100 26.7325 27.4550 28.1775
28.9000 30.3450 31.7900 33.2350 34.6800 37.5700
40.4600 43.3500 46.2400 52.0200 57.8000 63.5800
69.3600 80.9200 92.4800 104.0400 115.6000 137.2750
158.9500 180.6250 202.3000 223.9750 245.6500 267.3250
289.0000
T MESH 9.
0.0000 22.5000 45.0000 67.5000 90.0000 112.5000
135.0000 157.5000 180.0000
GEOMETRY 991.
.0000 30.3450 135.0000 -.999994 -.003517 .000180
.0007 26.7325 0.0000 -.999799 -.020028 -.000012
.0009 28.9000 90.0000 -.999471 .032450 -.002328
.0029 27.4550 45.0000 -.994741 .102286 -.005338
.0078 28.1775 67.5000 -.992455 .122305 -.008609
.0099 26.7325 22.5000 -.994329 -.106305 .003078
.0532 30.3450 157.5000 -.980441 -.196739 .005447
.0778 31.7900 180.0000 -.974464 .224543 -.000008
.0863 27.4550 67.5000 -.952733 -.303124 .020380
.0915 30.3450 180.0000 -.969981 -.243179 .000017
.0998 30.3450 112.5000 -.956383 .291323 -.021508
.1025 28.1775 90.0000 -.951889 -.305643 .022149
.1171 26.7325 45.0000 -.927748 -.372725 .018954
.1242 28.9000 112.5000 -.950576 -.309804 .020656
.1298 31.7900 157.5000 -.956120 .292836 -.008981
.1550 27.4550 22.5000 -.871558 .490069 -.014798
.1979 26.0100 0.0000 -.871352 -.490658 .000007
.2614 27.4550 0.0000 -.807477 .589899 -.000138
.2695 28.9000 67.5000 -.846628 .530655 -.040326

```

Figure 11. Part of Input File for Inlet Geometry Data Case

```

NACA 0012 AIRFOIL WING ALONE FINE MESH SEPT 21, 1982
M INF = 0.75 ALPHA =1.0 DEGREES
FREESTREAM
1.0      0.75      0.0      1.0
SWEEPS
800.0    200.0    60.0
0.1      0.1      0.1
ADI      3.0
IPRI
WING
SFLOW
1.0      1.0      1.0
X MESH      65.
-2.5000    -2.2500    -2.0000    -1.7500    -1.5000    -1.2500
-1.0000    -.8500     -.7000     -.5500     -.4000     -.3500
-.3000     -.2500     -.2000     -.1750     -.1500     -.1250
-.1000     -.0750     -.0500     -.0250     0.0000     .0250
.0500      .0750      .1000      .1375      .1750      .2125
.2500      .3000      .3500      .4000      .4500      .5000
.5500      .6000      .6500      .7000      .7500      .8000
.8500      .8844      .9188      .9531      .9875      1.0125
1.0375     1.0625     1.0875     1.1031     1.1188     1.1344
1.1500     1.1875     1.2250     1.2625     1.3000     1.3750
1.4500     1.5250     1.6000     -3.0000     -2.75000
Y MESH      9.
-.2000     -.1500     -.1000     -.0500     0.0000     .0500
.1000      .1500      .2000
Z MESH      61.
-5.0000    -4.5000    -4.0000    -3.5000    -3.0000    -2.5000
-2.0000    -1.7500    -1.5000    -1.2500    -1.0000    -.9000
-.8000     -.7000     -.6000     -.5250     -.4500     -.3750
-.3000     -.2625     -.2250     -.1875     -.1500     -.1219
-.0938     -.0656     -.0375     -.0125     .0125     .0375
.0625      .0844      .1063      .1281      .1500     .1875
.2250      .2625      .3000      .3750      .4500     .5250
.6000      .7000      .8000      .9000      1.0000     1.2500
1.5000     1.7500     2.0000     2.5000     3.0000     3.5000
4.0000     4.5000     5.0000     5.5000     6.0000     -6.0000
-5.5000
GEOMETRY 495.
0.0000     -.2000     0.0000    -1.000000    0.000000    0.000000
0.0000     -.1500     0.0000    -1.000000    0.000000    0.000000
0.0000     -.1000     0.0000    -1.000000    0.000000    0.000000
0.0000     -.0500     0.0000    -1.000000    0.000000    0.000000
0.0000     0.0000     0.0000    -1.000000    0.000000    0.000000
0.0000     .0500     0.0000    -1.000000    0.000000    0.000000
0.0000     .1000     0.0000    -1.000000    0.000000    0.000000
0.0000     .1500     0.0000    -1.000000    0.000000    0.000000
0.0000     .2000     0.0000    -1.000000    0.000000    0.000000
.0053     -.2000     -.0125    -.760089    0.000000    -.649819
.0053     -.1500     -.0125    -.760089    0.000000    -.649819
.0053     -.1000     -.0125    -.760089    0.000000    -.649819
.0053     -.0500     -.0125    -.760089    0.000000    -.649819
.0053     0.0000     -.0125    -.760089    0.000000    -.649819
.0053     .0500     -.0125    -.760089    0.000000    -.649819
.0053     .1000     -.0125    -.760089    0.000000    -.649819
.0053     .1500     -.0125    -.760089    0.000000    -.649819
.0053     .2000     -.0125    -.760089    0.000000    -.649819
.0053     -.2000     .0125     -.760089    0.000000    .649819
.0053     -.1500     .0125     -.760089    0.000000    .649819

```

Figure 12. Part of Input File for NACA-0012 Airfoil Analysis

```

NASA PLANK WING, PYLON AND NACELLE 11/09/83 77 X 41 X 65 MESH
CONF. 5 M INF =0.20 ALPHA = 5.0 DEGREES M C.F. = 0.10
FREESTREAM
1.0 0.2 0.0 5.0
CFACE
-4.1 .1
SWEEPS
800.0 200.0 100.0
1.0 1.0 1.0
WING
SFLOW
1.0 1.0 1.0
XMESH 77.
-20.0000 -18.0000 -16.0000 -12.0000 -11.0000 -10.0000
-9.5000 -9.0000 -8.7000 -8.4000 -8.1000 -7.8000
-7.5000 -7.0000 -6.5000 -6.0000 -5.5000 -5.0000
-4.7000 -4.4000 -4.1000 -3.8000 -3.5000 -3.0000
-2.5000 -2.0000 -1.7500 -1.5000 -1.2500 -1.0000
-.7500 -.5000 -.2500 .0100 .2500 .5000
.7500 1.0000 1.2500 1.5000 2.0000 2.5000
3.0000 3.5000 4.0000 4.5000 5.0000 5.2500
5.5000 5.7500 6.0000 6.2500 6.5000 7.0000
7.5000 8.0000 8.2500 8.5000 8.7000 8.9000
9.1000 9.3000 9.5000 9.7000 9.9000 10.1000
10.3000 10.5000 11.0000 11.5000 12.0000 12.5000
13.0000 14.0000 15.0000 18.0000 20.0000
YMESH 41.
-20.0 -16.5 -13.5 -11.0 -9.0 -6.75
-5.5 -4.0 -3.0 -2.5 -2.25 -2.0
-1.75 -1.5 -1.25 -1.0 -.86 -.64
-.42 -.21 0.0 .21 .42 .64
.86 1.0 1.25 1.5 1.75 2.0
2.25 2.5 3.0 4.0 5.5 6.75
9.0 11.0 13.5 16.5 20.0
ZMESH 65.
72.0000 -56.0000 -43.0000 -40.0000 -32.0000 -28.0000
-24.0000 -20.0000 -16.0000 -14.0000 -12.0000 -10.0000
-8.0000 -7.0000 -6.5000 -6.0500 -5.7000 -5.3500
-5.0000 -4.6500 -4.3000 -3.9750 -3.6500 -3.3250
-3.0000 -2.6750 -2.3500 -2.0250 -1.7000 -1.5000
-1.3000 -1.1000 -.9000 -.6750 -.4500 -.2250
0.0000 .2250 .4500 .6750 .9000 1.2000
1.5000 1.8000 2.1000 2.5000 3.0000 3.5000
4.0000 5.0000 6.0000 7.0000 8.0000 10.0000
12.0000 14.0000 16.0000 20.0000 24.0000 28.0000
32.0000 40.0000 48.0000 56.0000 64.0000
GEOM 8047.
-8.4996 -1.2500 -5.7000 -.986797 -.107550 -.121093
-8.4996 1.2500 -5.7000 -.986797 .107550 -.121093
-8.4966 -1.7500 -5.0000 -.913084 -.378550 -.151583
-8.4966 1.7500 -5.0000 -.913084 .378550 -.151583
-8.4783 -1.0000 -2.6750 -.618839 -.408998 .670641
-8.4783 1.0000 -2.6750 -.618839 .408998 .670641
-8.4000 -1.9175 -4.3000 -.354548 -.935038 0.000000
-8.4000 -1.9192 -3.9750 -.354086 -.921370 .160315
-8.4000 -1.9147 -4.6500 -.354033 -.919222 -.172314
-8.4000 -1.8336 -3.6500 -.353535 -.881171 .313927
-8.4000 -1.8150 -5.0000 -.353499 -.872520 -.337264
-8.4000 -1.7500 -5.1497 -.353505 -.842197 -.407110
-8.4000 -1.7500 -3.4503 -.353505 -.842197 .407110

```

Figure 13. Part of Input File for Wing-Pylon-Nacelle Geometry

## 5.2 INPUT RECOMMENDATIONS

Mesh selection is probably the most important step in obtaining accurate flowfield predictions for a given analysis problem. There are two primary reasons for this situation. The first reason is the limitation on the maximum number of grid lines and surface-grid intersects due to computer memory size and the way the analysis was coded (see Section 5.1.3). In theory, as the mesh spacing becomes very small, the solution of the difference equations should approach the solution of the partial differential equations. Thus, in the limit, as the mesh spacing becomes very small, the solution is independent of mesh. Unfortunately, for most problems of interest this limit is of no consequence because the meshes that can be used are very coarse, in fact barely adequate in many cases.

A second consideration in mesh selection is convergence rate. Solutions using uniform meshes converge fastest with least possibility of instability. However, for most problems, given the limitation of maximum number of grid lines, uniform meshes give unacceptable accuracy. Hence, grid lines must be packed in areas of interest (i.e., rapid flow changes) in order to resolve the flowfield. The mesh can be sparser far from the body where the flow properties vary slowly with position. This packing has to be accomplished with discretion or the solution can fail to converge.

The following discussion can be used as a guide for mesh placement.

Ground rules for mesh selection are:

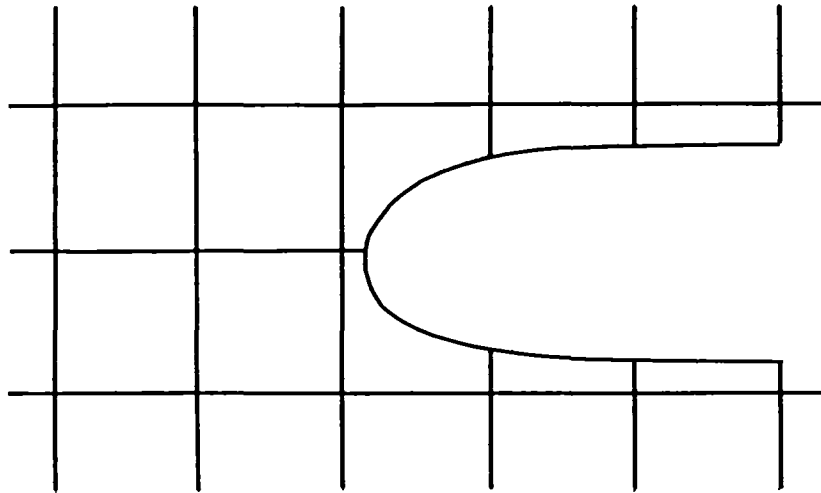
- o Sufficient mesh are required to resolve the geometry and flowfield in critical regions (fig. 14).
- o Mesh spacing should vary gradually from one region to another (fig. 15). Adjacent grid spacings should differ by no more than a factor of two within any mesh level.
- o Mesh aspect ratios,  $\Delta x/\Delta y$ ,  $\Delta x/\Delta z$ , etc., should be approximately one in important flow regions. This becomes even more important when the flow is transonic.
- o The edges of the computational volume must be located far enough from the bodies that they do not greatly affect the flowfield. That is, the flow in the vicinity of the edges of the computational volume can be reasonably approximated by freestream conditions.

As an example, a nondimensional mesh for calculation of the flowfield around a typical turbofan engine inlet is shown in Figure 16 and tabulated in Table 2. What is shown is the coarsest (level 2) of a sequence of three meshes. The fine mesh (level 4) is generated by adding 3 mesh equally spaced between each of the given mesh.

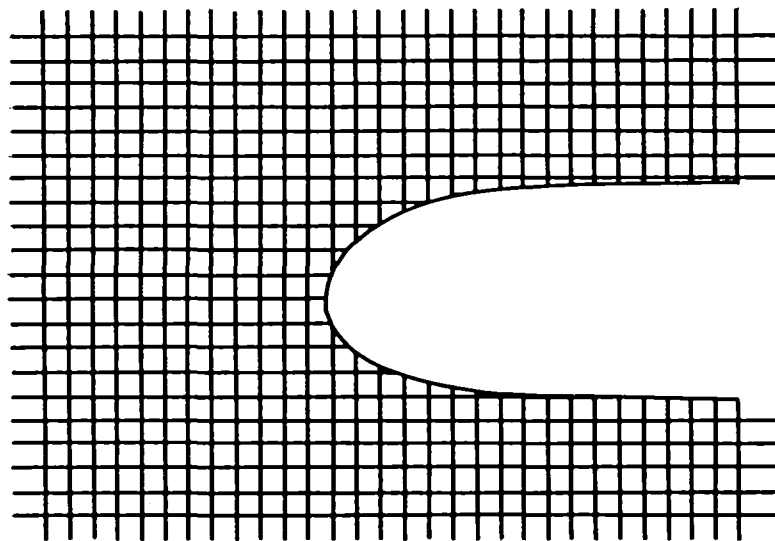
This mesh is a compromise between cost of a computation and accuracy. It is just adequate for making the calculation. It is safest to make the calculations with the number of theta mesh held constant for all three levels. Otherwise, for sample inlet calculations, there have been problems with the multigrid convergence.

It has been found during limited numerical experiments that for wing calculations it takes a minimum of 20 to 30 grid in the chordwise direction across a wing to obtain any kind of reasonable (though not extremely accurate) results.

Selection of mesh for other configurations is a difficult problem. The best advice would be to try several meshes and/or compare with experiments for similar configurations.

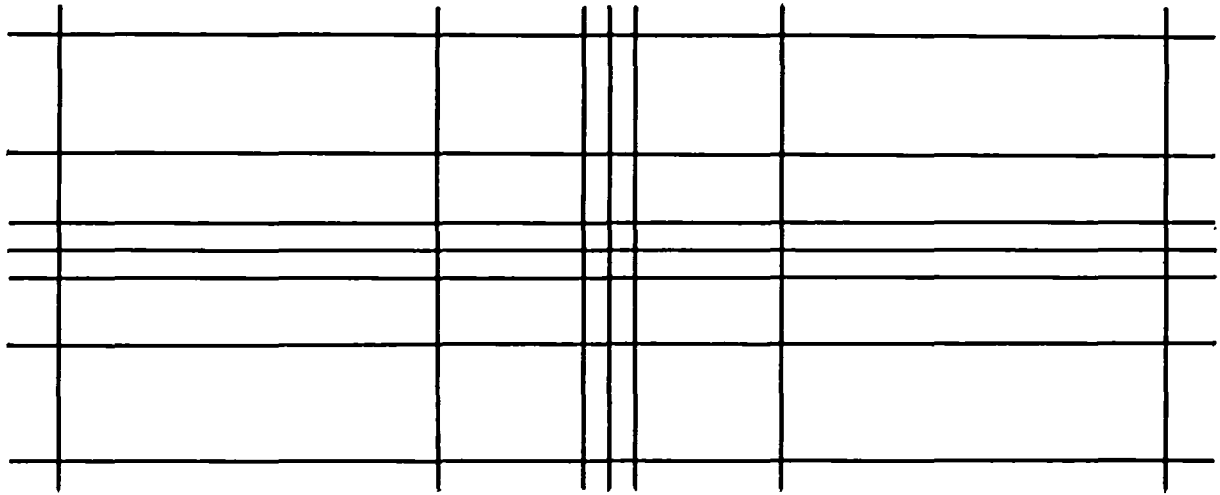


(a) Insufficient Mesh

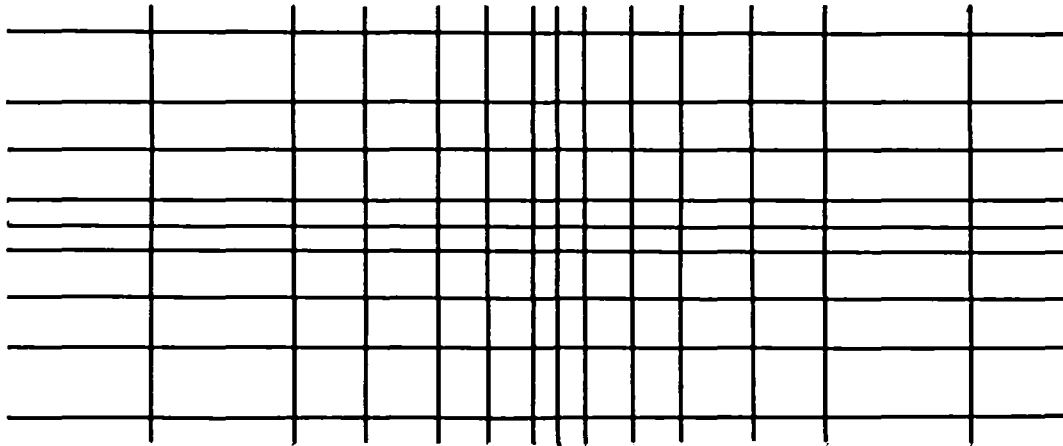


(b) Sufficient Mesh

*Figure 14. Mesh Density Required to Resolve Geometry Effects on Flowfield*



(a) Poor Spacing



(b) Recommended Mesh Spacing Variation

*Figure 15. Mesh Spacing Control*

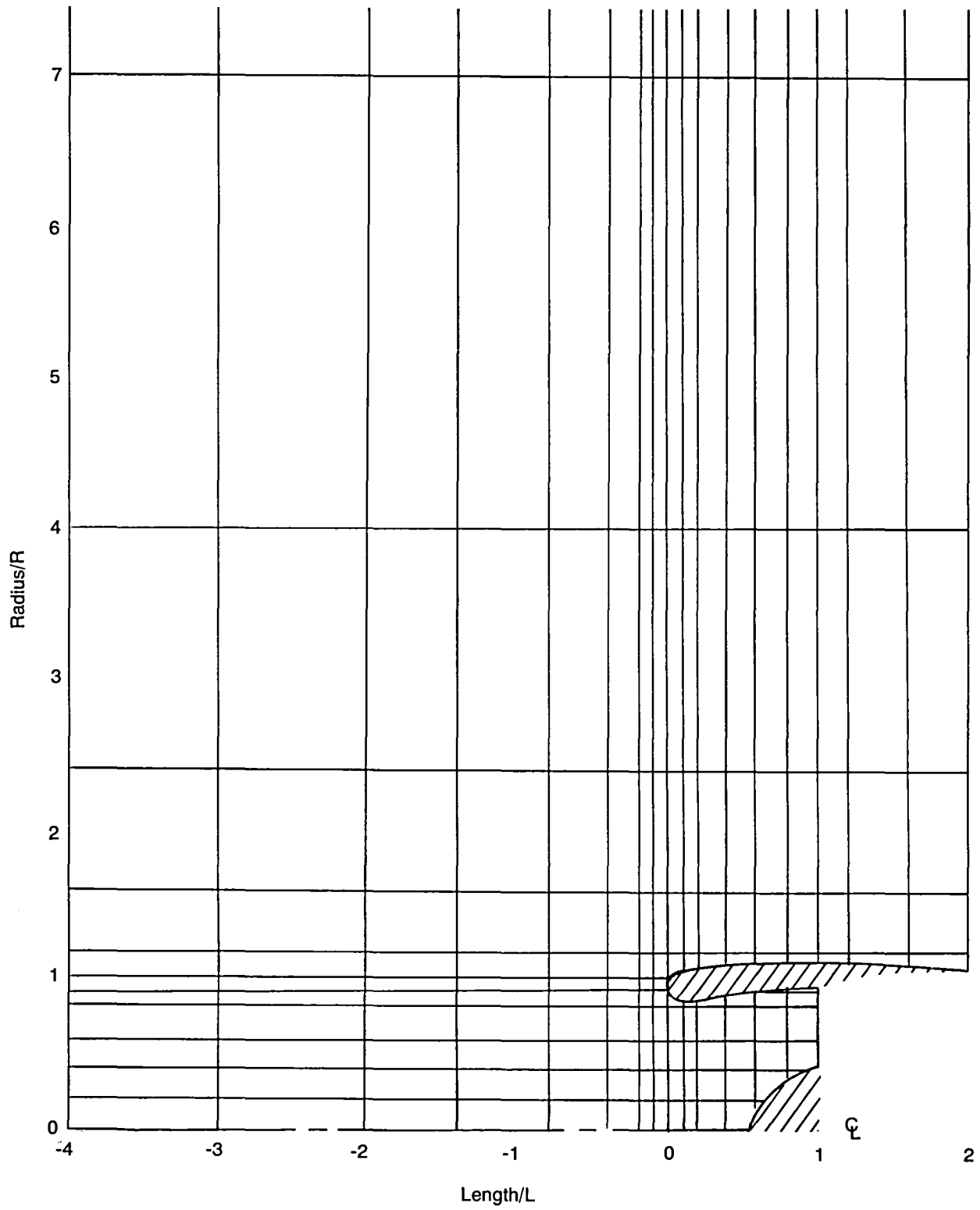


Figure 16. Standard Inlet Mesh (Coarse)



Table 2. Standard Inlet Mesh (Level 2)

	x/L		r/R		$\theta$ (degrees)
1	-4.0	1	0.0	1	0
2	-3.0	2	0.2	2	22.5
3	-2.0	3	0.4	3	45.0
4	-1.4	4	0.6	4	67.5
5	-0.8	5	0.8	5	90.0
6	-0.4	6	0.9	6	112.5
7	-0.2	7	1.0	7	135.0
8	-0.1	8	1.2	8	157.5
9	0.0	9	1.6	9	180.0
10	0.1	10	2.4	10	202.5
11	0.2	11	4.0	11	225.0
12	0.4	12	7.0	12	247.5
13	0.6	13	10.0	13	270.0
14	0.8			14	292.5
15	1.0			15	315.0
16	1.2			16	337.5
17	1.6				
18	2.0				

The program can make calculations using up to four levels. Every lower level is generated from the next higher level by deleting every other mesh line. The exception is for cylindrical coordinate computations where the theta (circumferential) grid can be held constant between levels. This option exists because of multigrid convergence problems (ref. 4) that have been noted with some geometries for cylindrical coordinates.

Multiple levels are used with multigrid to give orders of magnitude decreases in run costs by faster and less expensive convergence. In theory it is best to use many levels. In practice, problems occur at the lower (coarser mesh) levels because the mesh can become very sparse near the body(s) and fail to resolve geometry features. For problems that use only about 50 000 to 70 000 grid intersects, three levels are all that should be used. If problems with convergence seem to be occurring between levels 2 and 3, then two levels may be used.

The code is most stable when the flow is subsonic. More problems have been noticed for transonic flow and the possibility of problems increases with the maximum Mach numbers. The code usually works for transonic flows, but occasionally it will fail. If it fails, recommendations include:

- o Check that a physically realistic problem is being run.
- o Lower the freestream or compressor face Mach number if possible.
- o Try an alternate grid with a squarer mesh in the region of difficulty.
- o Experiment by moving mesh around.

The surface geometry must be complete (closed) or end on a computational boundary. That is, a surface cannot just end in the middle of the flowfield. A closed surface such as a wing or sphere is acceptable. Computational boundaries are defined by the compressor face and the smallest and largest value for each mesh. Geometry cannot extend beyond or through the computational boundaries.

An inlet diffuser geometry must end at the compressor face. (This does not have to be the physical compressor face; the diffuser can be shortened or extended for computational purposes.)

### 5.3 PROGRAM OUTPUT

The computer code calculates the potential function and, hence, all flow properties at all nodes. These include mesh nodes as well as all intersections of the mesh with the surface. The quantity of possible output is very large, especially for a dense mesh. What is printed is controlled by the user with the input print options.

The default output includes headings, listings of many of the program input parameters, and lists of the options that have been selected. The actual mesh and number of surface points are listed for each level. If the geometry has a duct, an area table for the duct is printed. If a lifting surface calculation is being made, tables are printed of the geometry information for the trailing edge of the wing as determined by the program. The default output includes the complete iteration history of the run including timing information. After convergence is obtained or an iteration limit is reached, a mass flow table is printed if there is a duct in the flowfield. This table is a check on the solution. The computed mass flow at a cross section is compared to the value being enforced as the boundary condition at the duct exit. Next is the surface properties printed for every fourth cut of the surface, x constant cuts first followed by y (r) constant and z( $\theta$ ) constant cuts. Last is a summary of the convergence history.

A variety of additional output can be requested. A listing of the input surface coordinate and normal values can be obtained. This list can be either ordered as input or in the internal ordering the computer code uses. Lists can be obtained of surface points that are special cases. These include surface nodes that are also mesh nodes and pairs of surface points adjacent to the same field point in the same coordinate. The internal program maps can also be obtained. These are lists of surface points in order along constant coordinate cuts of the surface and include the program calculated arc length. The user has some control of the density of surface properties output. Printout of the flowfield solution can be requested. Surface properties can be requested to be printed in terms of an alternate coordinate system.

### **5.3.1 DESCRIPTION OF PRINTED OUTPUT**

Much of the printed output from the code is self explanatory. Tables 3 through 7 define some of the quantities in the printout.

### **5.3.2 SAMPLE OUTPUT**

The sample output presented in Figure 17 is for a two-dimensional airfoil, NACA-0012, run as a test case for checking the Kutta condition implementation in the code. This is a very simple geometry, but it makes a good example for the program output. Only a small representative selection is presented. This run was made on the Cyber 203 at the NASA-Langley Research Center. The answers are the same using the CRAY-1. However, the timing and cost information on the Sweeping History table would be different.

## **5.4 DIAGNOSTICS AND TROUBLESHOOTING**

Many factors can cause difficulties with a computation. If no results are obtained, it is obvious there is a problem. In many ways, a more serious problem occurs when results are obtained that, to casual observation, appear reasonable but are, in fact, incorrect. Errors include bad inputs, inputs inconsistent with code limitations, logic errors in the code, poor choice of mesh, and wrong flow model, to name some possibilities. Some possible problems will be discussed and some of the code diagnostics are listed and explained. Their order is approximately that in which items are processed in the code.

The best way to be sure that the program is providing acceptable answers is to use the code on similar problems for which experimental results are available for comparison. If this is not possible, then the next best alternatives are as follows. Prepare sample plots of cross sections of the geometry with the mesh to be used. They should look reasonable. (See the discussion in Section 5.2 and Figures 14 and 15.) If they do not look reasonable, computed results will probably be poor. A table of computed mass flow is printed for ducts. This table is generated from the solution and is a check of the solution. Typical errors (leakage) are of the order of 1 to 2%. Much greater errors indicate an inadequate mesh and/or poor convergence. Another check is to see how quickly the solution changes relative to the mesh. Very large changes in velocity or flow direction between two mesh lines are an indication that a denser mesh is required.

### **5.4.1 INCORRECT INPUT OTHER THAN GEOMETRY**

The first thing done by the program is to read the input cards. These are processed group by group. If the input is not formatted correctly the program will get "out of step" and expect a keyword where there is none. The message

Table 3. Headings for Surface Point and Surface Geometry Printout

INDEX	Surface point index
X	x
Y or R	y or r
Z or THETA	z or $\theta$
S	s, arc length along cut
NX	$n_x$ , component of unit surface normal
NY or NR	$n_y$ or $n_r$ , component of unit surface normal
NZ or NT	$n_z$ or $n_\theta$ , component of unit surface normal
I } J } K }	indices of the mesh lines defining the field point adjacent to the surface point
SURFARM	$\Delta x$ , $\Delta y$ , $\Delta r$ , $\Delta z$ or $\Delta\theta$ between surface point and adjacent field point
TYPE	$\left\{ \begin{array}{l} -1 = x \text{ intersect} \\ 0 = z \text{ or theta intersect} \\ 1 = y \text{ or r intersect} \\ 2 = \text{both mesh and surface node} \end{array} \right.$

Table 4. Convergence History Headings

SWEEP	Relaxation sweep number, (n)
**FIELD POINTS**	
AVE RESIDUE	Sum of $ \phi_{i,j,k}^{(n)} - \phi_{i,j,k}^{(n-1)} $ over all points i,j,k in the flowfield divided by $\phi_{\max}^{(n)} - \phi_{\min}^{(n)}$ and the number of such field points
I } J } K }	$\left\{ \begin{array}{l} \text{The indices i,j,k of the field point having the maximum change in } \phi \text{ and the maximum value of} \\  \phi_{i,j,k}^{(n)} - \phi_{i,j,k}^{(n-1)}  \text{ divided by } \phi_{\max}^{(n)} - \phi_{\min}^{(n)} \end{array} \right.$
MAX RESIDUE	
"CONVERGING/ DIVERGING"	** , MAX RESIDUE decreasing, or *** , MAX RESIDUE increasing
**SURFACE POINTS**	
AVE RESIDUE	Sum of $ \phi_S^{(n)} - \phi_S^{(n-1)} $ over all surface points S divided by $\phi_{\max}^{(n)} - \phi_{\min}^{(n)}$ and the number of surface points
I } J } K } INDEX MAX RESIDUE	$\left\{ \begin{array}{l} \text{The mesh indices i,j,k of the field point next to the surface point with the maximum change in } \phi, \text{ the index of that surface point, and the maximum value of }  \phi_S^{(n)} - \phi_S^{(n-1)}  \text{ divided by } \phi_{\max}^{(n)} - \phi_{\min}^{(n)} \end{array} \right.$
M > 1.0	number of field points for which Mach number > 1.0
EIGEN1	$1/(1-\lambda_1)$ , see ref. 1
EIGEN2	$1/(1-\lambda_2)$ , see ref. 1
"EXTRAPOLATION FLAG"	* indicates flowfield extrapolation was made after this sweep

Table 5. Surface Point Printout Headings

INDEX	Surface point number
X	x
Y or R	y or r
Z or THETA	z or $\theta$
S	s, arc length along the cut of the surface
MACH	Mach Number
CP	$C_p$ , coefficient of pressure, $(p/p_\infty - 1)/(1/2\gamma M_\infty^2)$ (if $M_\infty = 0.0$ , then $C_p = (p/p^* - 1)/(1/2\gamma)$ , where the * indicates sonic conditions)
PHI	$\phi$ , potential function
Q	$q = (u^2 + v^2 + w^2)^{1/2} = (u^2 + u_r^2 + u_\theta^2)^{1/2}$
PHI,S	$u_s$ , component of velocity along the cut
U	u, axial velocity component
V or U-RADIAL	v or $u_r$ , velocity component
W or U-THETA	w or $u_\theta$ , velocity component

Table 6. Field Point Printout Headings

Y or R	y or r
MACH	Mach Number
PHI	$\phi$ , potential function
CP	$C_p$ , coefficient of pressure, $(p/p_\infty - 1)/(1/2\gamma M_\infty^2)$ (if $M_\infty = 0.0$ , then $C_p = (p/p^* - 1)/(1/2\gamma)$ , where the * indicates sonic conditions)
U	u, axial velocity component
V	v, y component of velocity
W	w, z component of velocity
U-RADIAL	$u_r$ , radial velocity component
U-THETA	$u_\theta$ , circumferential velocity component

Table 7. Headings for Kutta Boundary Condition Printout

N	Jump number
SURFACE	Surface number
SEQ. NO.	Sequence number of jump in order along cut
I	Index of last x = constant plane to cut trailing edge
J	Index of y = constant plane that cut is in
JJUMP	Index of first y mesh above trailing edge
K	Index of z = constant plane that cut is in
KJUMP	Index of first z mesh above trailing edge
NDEXL	Index of last surface point below the body on this cut which is not an x intersect
NDEXU	Index of last surface point above the body on this cut which is not an x intersect
DELPHI	$\Delta\phi = \Gamma$ at trailing edge
DPHICL	Calculated value of $\Gamma$ at trailing edge (used in multigrid cycling)
ITYPCJ	= 0 $\Gamma$ calculated directly = n $\Gamma$ interpolated from parameters on line n of interpolation table
JUMP INTERPOLATION INFORMATION	
N	Interpolation index
ITPIJP1 } ITPIJP2 } NDEXJP1 } NDEXJP2 } ETAJMP1 } ETAJMP2 }	$\Delta\phi = \text{ETAJMP1} \cdot \Gamma_1 + \text{ETAJMP2} \cdot \Gamma_2$ <p>where <math>\Gamma_i</math> is <math>\Gamma</math> of jump NDEXJPi where NDEXJPi is jump number. NDEXJPi refers to y constant cut table if ITPIJPi = 2, z constant table if ITPIJPi = 1.</p>

\*\*\*\*\* P 4 6 5 C - THREE-DIMENSIONAL TRANSONIC POTENTIAL FLOW PROGRAM \*\*\*\*\*

VERSION C00 - OCTOBER 11, 1983

RUN DATE - 10/25/83

ABSTRACT -

THIS IS A COMPUTER PROGRAM WRITTEN FOR THE CONTROL DATA CORPORATION CYBER 203 COMPUTER. ITS PURPOSE IS THE COMPUTATION OF TRANSONIC POTENTIAL FLOW ABOUT THREE DIMENSIONAL INLETS, DUCTS AND BODIES. IT IS PROGRAMMED IN CYBER 203 EXTENDED FORTRAN IV.

REFERENCES -

REYHNER, T. A., "TRANSONIC POTENTIAL FLOW COMPUTATION ABOUT THREE-DIMENSIONAL INLETS, DUCTS AND BODIES," AIAA JOURNAL, VOL. 19, SEPTEMBER 1981, PP. 1112-1121.

REYHNER, T. A., "COMPUTATION OF TRANSONIC POTENTIAL FLOW ABOUT THREE-DIMENSIONAL INLETS, DUCTS, AND BODIES," NASA CR-3514, MARCH 1982

PROPRIETARY NOTICE -

\*\*\*\*\*  
\* THE COMPUTER PROGRAM, P465 - VERSION C, IS THE SOLE PROPERTY OF THE BOEING COMMERCIAL AIRPLANE \*  
\* COMPANY UNTIL JANUARY 1, 1986 DURING WHICH TIME NASA (THE NATIONAL AERONAUTICS AND SPACE \*  
\* ADMINISTRATION) HAS RIGHTS OF USE \*  
\* \*\*\*\*\*

VERSION C -

VERY FINE MESH  
KUTTA CONDITION BOUNDARY CONDITION  
Y OR Z LINE RELAXATION  
4 LEVEL CALCULATIONS  
VERY COARSE GRID CAPABILITY

CONSULTATION -

T. A. REYHNER	BOEING COMMERCIAL AIRPLANE CO.	(206) 237-2519
R. G. JORSTAD	BOEING COMPUTER SERVICES, INC.	(206) 656-5745
D. E. REUBUSH	NASA LANGLEY RESEARCH-CENTER	(804) 865-2675

RUN TITLE -

NACA 0012 AIRFOIL WING ALONE FINE MESH SEPT 21, 1982  
M INF = 0.75 ALPHA = 1.0 DEGREES

(a) Sample Output

Figure 17. Sample Program Output

## THE FLOWFIELD PARAMETERS ARE -

A INF	"	1.00000	
Q INF	"	.75000	
ALPHA1 - ARCTAN(W INF/U INF)	"	.000	DEGREES
ALPHA2 - ARCTAN(W INF/U INF)	"	1.000	DEGREES
M INF	"	.750	
U INF	"	.74989	
V INF	"	.00000	
W INF	"	.01309	

WING OR WING LIKE GEOMETRY HAS BEEN SPECIFIED

## MESH AND CONVERGENCE PARAMETERS -

LEVEL NUMBER	2	3	4
NX	17	33	65
NY	3	5	9
NZ	16	31	61
MAXIMUM NUMBER OF SWEEPS	800	200	60
CONVERGENCE TEST VALUES *(10**6)	.1000	.1000	.1000
MAX. NUMBER OF SWEEPS PER VISIT	100	20	20
MAXIMUM NUMBER OF VISITS	10	20	4

ALTERNATING DIRECTION LINE RELAXATION (ADI) USED - ALTERNATING BETWEEN Y AND Z LINES.

MULTIGRID PROCEDURE WILL BE USED.

CARTESIAN COORDINATES WILL BE USED.

## SURFACE FLOW PROPERTIES PRINT REQUESTED -

X CONSTANT CUTS	X=X(I)	(I-1) DIVISIBLE BY	1
Y CONSTANT CUTS	Y=Y(J)	(J-1) DIVISIBLE BY	1
Z CONSTANT CUTS	Z=Z(K)	(K-1) DIVISIBLE BY	1

(b) Sample Output (Continued)

Figure 17. Sample Program Output



PRINTOUT REQUESTED ON INTERMEDIATE LEVELS.

THERE ARE 495 SURFACE POINTS. THE LIMIT IS 8500

MESH =

NX\*NY\*NZ = 35685 THIS DATA CASE USES 35685 OF THE AVAILABLE 252105, FIELD POINTS  
NY\*NZ = 549 THE LIMIT IS 4250  
NX\*NY = 585 THE LIMIT IS 8500  
NX\*NZ = 3965 THE LIMIT IS 8500

\*\*\*\*\*  
\*\*\*\*\* X MESH \*\*\*\*\*  
\*\*\*\*\*

1)	-3.0000	22)	-.0750	43)	.7500
2)	-2.7500	23)	-.0500	44)	.8000
3)	-2.5000	24)	-.0250	45)	.8500
4)	-2.2500	25)	.0000	46)	.8844
5)	-2.0000	26)	.0250	47)	.9188
6)	-1.7500	27)	.0500	48)	.9531
7)	-1.5000	28)	.0750	49)	.9875
8)	-1.2500	29)	.1000	50)	1.0125
9)	-1.0000	30)	.1375	51)	1.0375
10)	-.8500	31)	.1750	52)	1.0625
11)	-.7000	32)	.2125	53)	1.0875
12)	-.5500	33)	.2500	54)	1.1031
13)	-.4000	34)	.3000	55)	1.1188
14)	-.3500	35)	.3500	56)	1.1344
15)	-.3000	36)	.4000	57)	1.1500
16)	-.2500	37)	.4500	58)	1.1875
17)	-.2000	38)	.5000	59)	1.2250
18)	-.1750	39)	.5500	60)	1.2625
19)	-.1500	40)	.6000	61)	1.3000
20)	-.1250	41)	.6500	62)	1.3750
21)	-.1000	42)	.7000	63)	1.4500
				64)	1.5250
				65)	1.6000

(c) Sample Output (Continued)

Figure 17. Sample Program Output

\*\*\*\*\*  
 \*\*\*\*\* Y MESH \*\*\*\*\*  
 \*\*\*\*\*

1)	-.2000	4)	-.0500	7)	.1000
2)	-.1500	5)	.0000	8)	.1500
3)	-.1000	6)	.0500	9)	.2000

\*\*\*\*\*  
 \*\*\*\*\* Z MESH \*\*\*\*\*  
 \*\*\*\*\*

1)	-6.0000	21)	-.3000	41)	.3000
2)	-5.5000	22)	-.2625	42)	.3750
3)	-5.0000	23)	-.2250	43)	.4500
4)	-4.5000	24)	-.1875	44)	.5250
5)	-4.0000	25)	-.1500	45)	.6000
6)	-3.5000	26)	-.1219	46)	.7000
7)	-3.0000	27)	-.0938	47)	.8000
8)	-2.5000	28)	-.0656	48)	.9000
9)	-2.0000	29)	-.0375	49)	1.0000
10)	-1.7500	30)	-.0125	50)	1.2500
11)	-1.5000	31)	.0125	51)	1.5000
12)	-1.2500	32)	.0375	52)	1.7500
13)	-1.0000	33)	.0625	53)	2.0000
<del>14)</del>	<del>-.9000</del>	<del>34)</del>	<del>.0875</del>	<del>54)</del>	<del>2.5000</del>
15)	-.8000	35)	.1063	55)	3.0000
16)	-.7000	36)	.1291	56)	3.5000
<del>17)</del>	<del>-.6000</del>	<del>37)</del>	<del>.1500</del>	<del>57)</del>	<del>4.0000</del>
18)	-.5250	38)	.1875	58)	4.5000
19)	-.4500	39)	.2250	59)	5.0000
20)	-.3750	40)	.2625	60)	5.5000
				61)	6.0000

INPUT PROCESSING COMPLETED

THE FOLLOWING SURFACE POINTS ARE NOT ADJACENT TO FIELD POINTS

INDEX	X	Y	Z	NX	NY	NZ	TYPE
19	.000000	-.200000	.000000	-1.00000000	.00000000	.00000000	0
20	.000000	-.150000	.000000	-1.00000000	.00000000	.00000000	0
21	.000000	-.100000	.000000	-1.00000000	.00000000	.00000000	0
22	.000000	-.050000	.000000	-1.00000000	.00000000	.00000000	0
23	.000000	.000000	.000000	-1.00000000	.00000000	.00000000	0
24	.000000	.050000	.000000	-1.00000000	.00000000	.00000000	0
25	.000000	.100000	.000000	-1.00000000	.00000000	.00000000	0
26	.000000	.150000	.000000	-1.00000000	.00000000	.00000000	0
27	.000000	.200000	.000000	-1.00000000	.00000000	.00000000	0

(d) Sample Output (Continued)

Figure 17. Sample Program Output

KUTTA CONDITION JUMP INFORMATION -

JUMPS LYING IN Y CONSTANT CUTS

N	SURFACE	SEQ. NO.	I	J	KJUMP	NDEXL	NDEXU	ITYPCJ
1	0	0	49	1	31	469	478	0
2	0	0	49	2	31	470	479	0
3	0	0	49	3	31	471	480	0
4	0	0	49	4	31	472	481	0
5	0	0	49	5	31	473	482	0
6	0	0	49	6	31	474	483	0
7	0	0	49	7	31	475	484	0
8	0	0	49	8	31	476	485	0
9	0	0	49	9	31	477	486	0

(e) Kutta Boundary Condition Geometry Table

Figure 17. Sample Program Output

CONVERGENCE HISTORY		LEVEL NUMBER 4				VISIT NUMBER 3							
.....FIELD POINTS.....		.....SURFACE POINTS.....											
SWEEP	AVE RESIDUE	I	J	K	MAX RESIDUE	AVE RESIDUE	I	J	K INDEX	MAX RESIDUE	M>1	EIGEN1	EIGEN2
532	.20657E-06	34	1	41	-.67916E-05	..	.44027E-06	34	1 33 190	-.59000E-05	378	.10000E+01	.10000E+01
533	.73068E-07	34	5	33	.61222E-05	**	.45603E-06	34	5 33 194	.51122E-05	378	.10000E+01	.10000E+01
534	.12337E-06	34	1	35	.61124E-05	**	.27221E-06	33	1 33 172	.42597E-05	378	.10000E+01	.10000E+01
535	.67958E-07	34	5	33	.62691E-05	***	.36198E-06	34	5 33 194	.54313E-05	378	.31765E+01	.51287E-01
536	.11635E-06	34	1	34	.63610E-05	***	.22088E-06	34	1 33 190	.57858E-05	378	.14594E+02	-.30942E+02
537	.63708E-07	34	5	33	.60643E-05	**	.30031E-06	34	5 33 194	.52171E-05	378	.15583E+02	-.28264E+03

CONVERGENCE CRITERION SATISFIED ON LEVEL 4 VISIT 3

(f) Sample of Convergence History

Figure 17. Sample Program Output

## KUTTA CONDITION JUMP INFORMATION -

## JUMPS LYING IN Y CONSTANT CUTS

N	SURFACE	SEQ. NO.	I	J	KJUMP	NDEXL	NDEXU	ITYPCJ	DELPHI	DPHICL	DPHICR
1	1	1	49	1	31	469	478	0	.064593	.064593	.000000
2	1	2	49	2	31	470	479	0	.064593	.064593	.000000
3	1	3	49	3	31	471	480	0	.064593	.064593	.000000
4	1	4	49	4	31	472	481	0	.064592	.064592	.000000
5	1	5	49	5	31	473	482	0	.064592	.064592	.000000
6	1	6	49	6	31	474	483	0	.064592	.064592	.000000
7	1	7	49	7	31	475	484	0	.064593	.064593	.000000
8	1	8	49	8	31	476	485	0	.064593	.064593	.000000
9	1	9	49	9	31	477	486	0	.064593	.064593	.000000

(g) Kutta Boundary Condition  $\Gamma$  Table

Figure 17. Sample Program Output

SURFACE FLOW PROPERTIES -

Y = CONSTANT CUTS

INDEX	X	Y	Z	S	MACH	CP	PHI	Q	PHI,S	U	V	W
469	.9875	-.2000	-.6030	.0000	.6222	.3014	3.0156	.6322	-.6322	.6263	.0002	.0866
451	.9531	-.2000	-.0077	.0347	.6680	.1950	2.9929	.6751	-.6751	.6692	-.0001	.0888
433	.9188	-.2000	-.0125	.0694	.7049	.1078	2.9688	.7091	-.7091	.7034	-.0000	.0895
415	.8844	-.2000	-.0164	.1040	.7285	.0515	2.9438	.7306	-.7306	.7252	.0000	.0896
397	.8500	-.2000	-.0205	.1386	.7464	.0086	2.9182	.7468	-.7468	.7417	.0000	.0871
379	.8000	-.2000	-.0262	.1889	.7684	-.0440	2.8801	.7664	-.7664	.7618	-.0000	.0844
361	.7500	-.2000	-.0316	.2392	.7879	-.0910	2.8411	.7838	-.7838	.7796	-.0000	.0812
343	.7000	-.2000	-.0366	.2895	.8061	-.1347	2.8013	.7998	-.7998	.7961	-.0000	.0774
325	.6911	-.2000	-.0375	.2984	.8092	-.1422	2.7941	.8026	-.8026	.7989	-.0000	.0767
307	.6500	-.2000	-.0413	.3397	.8235	-.1766	2.7607	.8151	-.8151	.8118	-.0000	.0731
289	.6000	-.2000	-.0456	.3899	.8411	-.2187	2.7194	.8304	-.8304	.8276	-.0000	.0680
271	.5500	-.2000	-.0495	.4400	.8593	-.2621	2.6774	.8460	-.8460	.8437	-.0000	.0619
253	.5000	-.2000	-.0529	.4902	.8782	-.3072	2.6346	.8622	-.8622	.8604	-.0000	.0543
235	.4500	-.2000	-.0558	.5402	.8979	-.3540	2.5910	.8789	-.8789	.8777	-.0000	.0450
217	.4000	-.2000	-.0580	.5903	.9186	-.4028	2.5466	.8962	-.8962	.8956	-.0000	.0334
199	.3500	-.2000	-.0595	.6403	.9400	-.4529	2.5013	.9140	-.9140	.9138	-.0000	.0188
181	.3000	-.2000	-.0600	.6903	.9604	-.5003	2.4552	.9307	-.9307	.9307	-.0000	-.0000
163	.2500	-.2000	-.0594	.7403	.9766	-.5376	2.4082	.9439	-.9439	.9436	-.0000	-.0239
145	.2125	-.2000	-.0580	.7778	.9829	-.5522	2.3727	.9491	-.9491	.9479	-.0000	-.0463
127	.1750	-.2000	-.0557	.8154	.9812	-.5482	2.3370	.9477	-.9477	.9448	-.0000	-.0735
109	.1375	-.2000	-.0521	.8531	.9672	-.5160	2.3014	.9363	-.9363	.9301	-.0000	-.1072
91	.1000	-.2000	-.0468	.8910	.9370	-.4460	2.2662	.9115	-.9115	.8988	-.0000	-.1519
73	.0750	-.2000	-.0420	.9164	.9039	-.3680	2.2433	.8839	-.8839	.8831	-.0000	-.1903
37	.0567	-.2000	-.0375	.9353	.8602	-.2644	2.2269	.8468	-.8468	.8163	.0001	-.2255
55	.0500	-.2000	-.0356	.9422	.8314	-.1955	2.2210	.8220	-.8220	.7867	.0001	-.2382
19	.0250	-.2000	-.0262	.9690	.6543	.2269	2.2003	.6624	-.6624	.5983	.0003	-.2842
1	.0053	-.2000	-.0125	.9932	.2353	1.0091	2.1867	.2469	-.2469	.1604	-.0001	-.1976
10	.0053	-.2000	.0125	1.0200	.4023	.7595	2.1895	.4176	.4176	.2714	-.0003	.3174
28	.0250	-.2000	.0262	1.0441	.8046	-.1310	2.2064	.7985	.7985	.7213	.0003	.3426
64	.0500	-.2000	.0356	1.0709	.9908	-.5702	2.2307	.9554	.9554	.9145	.0002	.2768
46	.0567	-.2000	.0375	1.0778	1.0220	-.6409	2.2375	.9804	.9804	.9450	.0002	.2611
82	.0750	-.2000	.0420	1.0967	1.0691	-.7455	2.2564	1.0174	1.0174	.9935	.0001	.2191
100	.1000	-.2000	.0468	1.1221	1.0991	-.8102	2.2827	1.0404	1.0404	1.0258	.0001	.1733
118	.1375	-.2000	.0521	1.1600	1.1273	-.8701	2.3226	1.0617	1.0617	1.0547	.0002	.1215
136	.1750	-.2000	.0557	1.1977	1.1495	-.9164	2.3629	1.0783	1.0783	1.0751	.0001	.0836
154	.2125	-.2000	.0580	1.2353	1.1658	-.9498	2.4037	1.0903	1.0903	1.0890	-.0002	.0531
172	.2500	-.2000	.0594	1.2728	1.1739	-.9664	2.4448	1.0963	1.0963	1.0959	.0002	.0278
190	.3000	-.2000	.0600	1.3228	1.1586	-.9351	2.4997	1.0850	1.0850	1.0850	.0007	.0000
208	.3500	-.2000	.0595	1.3728	1.0574	-.7196	2.5533	1.0082	1.0082	1.0080	-.0001	-.0207
226	.4000	-.2000	.0580	1.4228	.9663	-.5139	2.6006	.9356	.9356	.9349	-.0000	-.0349
244	.4500	-.2000	.0558	1.4729	.9414	-.4562	2.6469	.9152	.9152	.9140	-.0000	-.0468
262	.5000	-.2000	.0529	1.5230	.9148	-.3939	2.6922	.8931	.8931	.8913	.0000	-.0563
280	.5500	-.2000	.0495	1.5731	.8900	-.3353	2.7364	.8722	.8722	.8699	.0000	-.0638
298	.6000	-.2000	.0456	1.6232	.8670	-.2804	2.7797	.8526	.8526	.8497	.0000	-.0698
316	.6500	-.2000	.0413	1.6734	.8452	-.2285	2.8220	.8339	.8339	.8305	.0000	-.0747
334	.6911	-.2000	.0375	1.7147	.8278	-.1869	2.8561	.8189	.8189	.8151	.0000	-.0783
352	.7000	-.2000	.0366	1.7236	.8241	-.1779	2.8634	.8156	.8156	.8118	-.0000	-.0790
370	.7500	-.2000	.0316	1.7739	.8027	-.1266	2.9039	.7969	.7969	.7926	-.0000	-.0825
388	.8000	-.2000	.0262	1.8242	.7802	-.0726	2.9435	.7770	.7770	.7723	-.0000	-.0856
406	.8500	-.2000	.0205	1.8745	.7556	-.0133	2.9821	.7550	.7550	.7498	-.0000	-.0881
424	.8844	-.2000	.0164	1.9091	.7358	.0340	3.0080	.7372	.7372	.7318	-.0000	-.0894
442	.9188	-.2000	.0125	1.9438	.7103	.0949	3.0332	.7140	.7140	.7083	-.0000	-.0901
460	.9531	-.2000	.0077	1.9784	.6713	.1871	3.0574	.6782	.6782	.6723	-.0001	-.0892
478	.9875	-.2000	.0030	2.0131	.6234	.2987	3.0802	.6333	.6333	.6274	.0002	-.0867

(h) Sample of Surface Properties Printout

Figure 17. Sample Program Output

\*\*\*\*\*  
 \*  
 \*\*\*\*\* SWEEPING HISTORY \*\*\*\*\*  
 \*  
 \*\*\*\*\*

LEVEL NO.	VISIT NO.	INITIAL SWEEP NO.	FINAL SWEEP NO.	TOTAL SWEEPS	** CHANGE IN PHI BETWEEN SWEEPS X (10**6) **				M>1	EXTRAP.	SECONDS PER SWEEP	OVERHEAD SECCNOS	WORK UNITS
					* AVERAGE * INITIAL	* AVERAGE * FINAL	* MAXIMUM * INITIAL	* MAXIMUM * FINAL					
2	1	1	100	100	43.1879	113.3141	-1096.8747	4703.2465	5	2	.071	1.881	8.659
3	1	101	120	20	100.1466	12.0684	1839.3208	-212.3870	40	0	.249	.130	4.899
2	2	121	220	100	76.2857	1.5660	408.4872	-16.1846	6	3	.074	.328	7.413
3	2	221	236	16	13.5406	2.3926	-233.3536	-68.2228	55	0	.250	.143	3.981
4	1	237	256	20	2.9514	.9189	-440.4125	-26.0873	378	0	1.037	.455	20.348
3	3	257	267	11	2.8198	3.2064	30.8287	22.2553	55	0	.255	1.182	3.823
2	3	268	367	100	10.6248	.8034	-57.2768	-7.9568	6	2	.074	.337	7.423
3	4	368	383	16	2.2223	.3438	21.6036	7.3227	55	0	.254	.143	4.034
4	2	384	403	20	.6295	.1873	-32.1730	-7.3376	387	0	1.038	.476	20.395
3	5	404	411	8	.6364	.4359	-3.7587	5.7691	55	0	.255	1.188	3.097
2	4	412	511	100	2.5285	.4190	-9.7500	5.5537	6	3	.074	.329	7.416
3	6	512	531	20	1.0744	.1037	-9.0064	-1.5826	55	0	.253	.143	5.005
4	3	532	537	6	.2066	.0637	-6.7916	6.0643	378	0	1.042	.476	6.457

\*\*\*\*\* TOTAL WORK UNITS (EQUIVALENT FINE MESH SWEEPS) = 102.951 \*\*\*\*\*

(i) Convergence History

Figure 17. Sample Program Output

THE FOLLOWING WAS NOT RECOGNIZED AS A KEYWORD THE PROGRAM WAS EXPECTING A KEYWORD THE NEXT CARDS ON THE INPUT FILE ARE -

is printed followed by the four characters not recognized and then the next twenty cards of the input file. The difficulty is usually in the previous input group. A common problem is the wrong number of intersects on the GEOM card (Card 1 for the GEOM input group).

The next step in the code is checking of many of the input quantities for reasonableness or values that are consistent with declared array lengths in the code. Most of these messages are self-explanatory. The following should help in interpreting some of the messages.

**NTMESH** See THET input group. Values must be consistent with the number of theta mesh specified with the TMESH group.

**NFFPR** See FLDT input group. NFFPR larger than declared array storage.

#### 5.4.2 GEOMETRY ERRORS

The next step in the code is the processing of the input geometry points. Bad points or missing points will cause fatal errors. The process of finding missing points can be quite difficult. The diagnostics and explanations are listed approximately in the order processed.

**EITHER THE FOLLOWING SURFACE POINTS ARE BAD OR THE INPUT MESH IS INCORRECT**

At least two of the three coordinate values for a surface point must be mesh values. That is because a surface point is defined as the intersection of a grid line with the surface, and a grid line is defined by two mesh values (for example,  $x=X(6)$ ,  $y=Y(8)$ ). Thus, either the point is not a surface intersect or a mistake has been made in input of the mesh values. Either remove the bad point(s) from the file or correct the input mesh.

**THE FOLLOWING SURFACE POINTS ARE NOT ADJACENT TO FIELD POINTS**

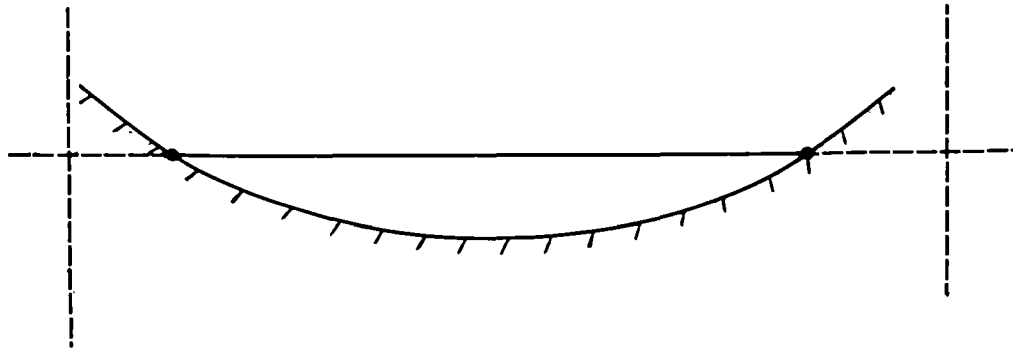
This is only an informative message, *not an error*. The situation is shown in Figure 18a. These points are not used in the calculations.

**THE FOLLOWING SURFACE POINTS ARE MULTIPLY ADJACENT IN THE SAME DIRECTION**

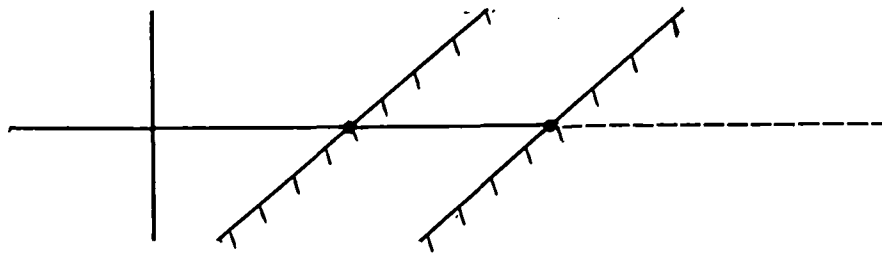
This is fatal geometry error and indicates a physically impossible situation. Examples are shown in Figures 18b and 18c. Figure 18b shows two overlapped surfaces. Figure 18c shows a physically correct geometry, but a surface intersect (the question mark) missing from the input file. Duplicate points would also draw this diagnostic. Another possible problem is a point that is correctly located, but the coordinates of the normal are bad, reversed in sign for example.

**THE FOLLOWING SURFACE POINTS ARE ADJACENT TO A ISURFTP( )=2 POINT AND/OR THERE ARE DUPLICATE POINTS**

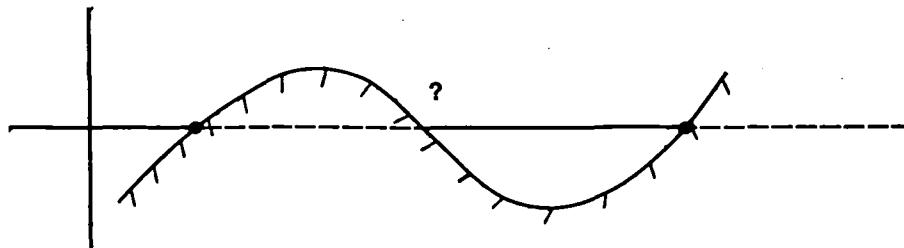
An ISURFTP( )=2 point is created (fig. 19a) when a mesh node and the surface coincide. There are several possibilities when this diagnostic occurs. If there are duplicate points, the correction is to eliminate the duplicate points. Another possibility is shown in Figure 19b where the surface is very near a mesh node. Normally, three points will be generated as shown, but one or more may be rounded to a ISURFTP( )=2 point. The correction is to delete the other one or two points, thus



**(a) Surface Points Not Adjacent to Mesh Nodes (Nonpoints)**



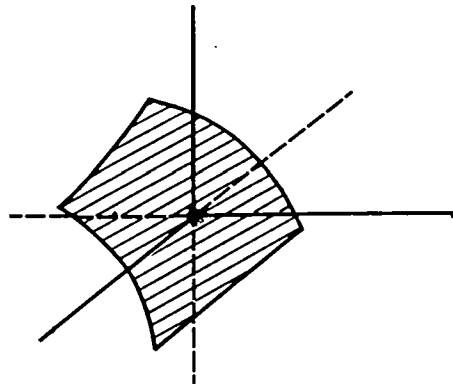
**(b) Two Points Adjacent to the Same Mesh Node**



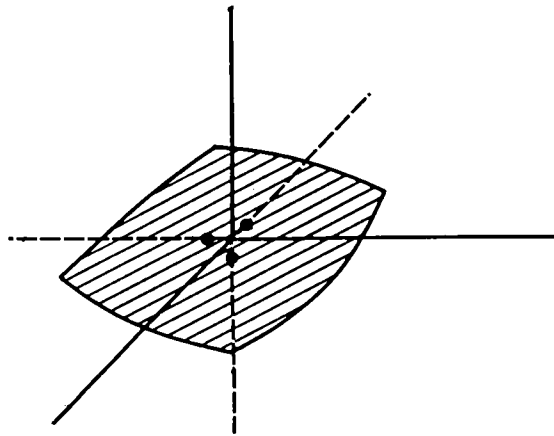
**(c) Two Points Adjacent to the Same Mesh Node**

*Figure 18. Possible Geometry Configurations and Errors*

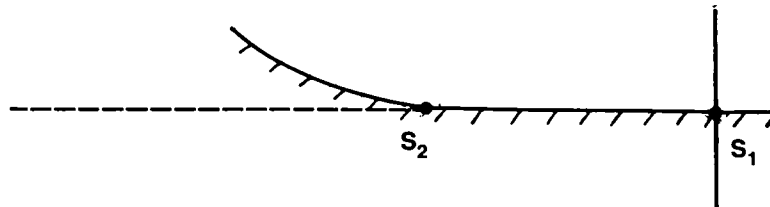




(a) ISURFTP ( ) = 2 Point, Mesh Node and Surface Coincide



(b) Almost ISURFTP ( ) = 2 Points



(c) ISURFTP ( ) = 2 Point ( $S_1$ ) and Point ( $S_2$ ) Adjacent to ISURFTP ( ) = 2 Point

Figure 19. ISURFTP ( ) = 2 Points and Possible Problems

moving the intersect to the mesh node. This is basically a tolerance problem in the geometry code. An additional possibility is shown in Figure 19c. For this situation, point  $S_2$  must be deleted from the input file. Other possibilities include configurations similar to Figures 19b and 19c. Once the situation is understood, the means of correction should be clear.

```

FATAL ERROR -   BITSET -   INCONSISTENT GEOMETRY
      X =           Y =           Z =
or
      X =           R =           THETA =
FATAL ERROR -   BITSET -- GEOMETRY PROBLEMS
      X = .....

```

BITSET, BITSET1 and BITSET2 are subroutines that sweep through the field and attempt to determine if mesh nodes are inside the flow or outside the flow (internal to a surface). Typical problems are missing points, extra points, and reversed normals. BITSET1 sweeps along y or radial lines, BITSET2 sweeps along z or circumferential lines. Normally, BITSET1 executes first and sets as many field nodes as possible. Then BITSET2 sweeps the other direction, checks for consistency with the BITSET1 results, and sets the remaining nodes. An extra pass is made with BITSET1 to ensure everything is consistent. BITSET1 and BITSET2 work on an x constant plane. BITSET compares adjacent x constant planes to insure they are consistent with each other and the surface intersects between them.

As an example, referring to Figure 20a, if point  $S_2$  is missing from the input file, an error will be detected by BITSET1 when point  $S_3$  is detected, and the coordinates printed will be that of mesh node  $P_3$ . If  $S_2$  is present, but the normal has the wrong sign, an error will be detected when  $S_2$  is encountered, and the coordinates printed will be those of  $P_2$ . If  $S_1$  is missing, the error may not be detected until BITSET2 executes.

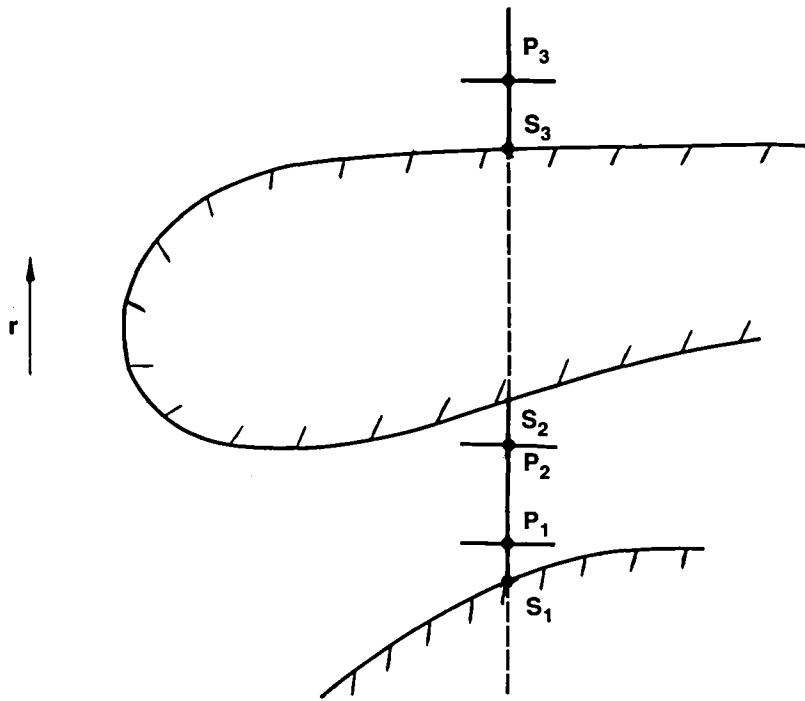
Referring to Figure 20b, if everything else is correct and point  $S_x$  is missing or the normals are bad, then BITSET will detect an error and the coordinates printed will be those of  $S_x$ , except that the x value printed will be  $x_2$ .

A problem that will cause error messages from BITSET, BITSET1 or BITSET2 is a configuration such as Figure 19b where a surface point is very near a mesh node. This configuration generates three surface points that are not all calculated simultaneously by the geometry code (ref. 7). It is possible that tolerances are such that one of these points can be found on the wrong side of the mesh node relative to the others. If this occurs, the simplest solution is to replace all three points by a single point located at the mesh node.

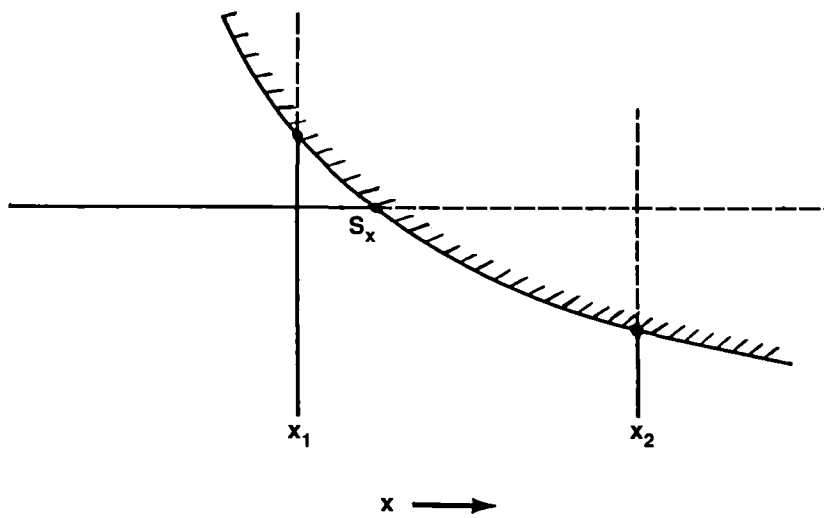
**A FATAL ERROR IN THE GEOMETRY DEFINITION HAS BEEN DETECTED.**

**ERROR DISCOVERED WHILE TRYING TO FOLLOW THE FOLLOWING CURVE**  
(followed by a list of surface points)

The computer program attempts to link the surface points in sequence along x, y, and z (x, r, and  $\theta$ ) cuts of the surface. This is done by starting at a point and finding the next ones in the sequence until a boundary is reached or the sequence has returned to the starting point forming a closed loop. If a boundary is reached, the search starts in the reverse direction from the initial point until another boundary is reached. A boundary is the edge of the computational field or the compressor face. If the search does not find a next point in the sequence and is not at a boundary, the preceding message is printed and the table of points found is printed. The points printed are in sequence starting at the initial point, except that if a boundary is reached and the search started in the reverse direction from the initial point, those points follow the boundary point



(a) Sample Geometry for BITSET1 and BITSET2 Error Explanation



(b) Sample Geometry for BITSET Error Explanation

Figure 20. Geometry for BITSET, BITSET1, and BITSET2 Explanations

without a break. The area of difficulty is at the end of the table. Typical problems are identical to those associated with the BITSET routines. They are missing points, bad or reversed normals, and points slightly out of place.

**SPECIAL SURFACE POINTS ON LEVEL \_\_\_\_\_  
MESH IS VERY COARSE**

This diagnostic occurs when two different surfaces are separated by only one grid line. The calculations in this region of the flowfield will be very inaccurate and also code failures can result. If the message occurs on levels 1 and 2, and the code appears to converge properly, the computation is probably all right. This is a warning message, not a fatal error.

### **5.4.3 CODE FAILURES**

The hardest part of getting the code to successfully run a data case has been getting geometry points that are complete and self-consistent. Code failures beyond that point are less frequent and often due to errors in the computer code. The other problems causing code failures once the geometry is correct include geometries the code cannot handle properly and supersonic flow. The program will compute transonic and potential flow most of the time, but large regions of supersonic flow can lead to convergence problems and code failure. Suggestions are to check inputs to make sure that the Mach numbers requested are physically reasonable and then see an analyst to determine if the code is at fault. The message

**FATAL ERROR - AA.LT.0.0 .....**

is associated with code failures. It means that the speed of sound has been calculated to be negative, indicating that physically impossible velocities have been computed.

**WARNING - AA.LT.0.0\_PLACES. THE PROGRAM WILL TRY TO RECOVER**

or

**WARNING - HIGH VELOCITY OUT OF SURFACE - RECOVERY WILL BE ATTEMPTED**

followed by values for the mesh indices and then coordinate values may be printed. The most common problem is a bad value for  $\phi$  obtained when interpolating up to a denser mesh for the first visit to the denser mesh. If the program recovers, that is, continues computing without further diagnostics, the run is probably okay.

Failure of the code to converge on lower levels is not very significant. Failure to converge on level 4 indicates results are suspect, but not necessarily incorrect.

### **5.4.4 OTHER PROBLEMS**

A problem with the multilevel calculations is the coarseness of the lowest grid level. There is code in the computer program to attempt to handle the very coarse meshes, but it is not always successful. A possible situation is shown in Figure 21. If this is the coarsest of four levels, there should be no problem with the final results if no problems develop on the coarsest mesh. If there are problems on the coarsest mesh, possible solutions are to use fewer levels or to add or move mesh.

Another source of difficulty is the logic for detecting the wing trailing edges and setting up the internal tables for calculations with a Kutta boundary condition. At present, this code does not work for all possible configurations, but it is usually possible to hand-correct these internal tables for a given flow problem. Consultation should be sought before this is attempted.

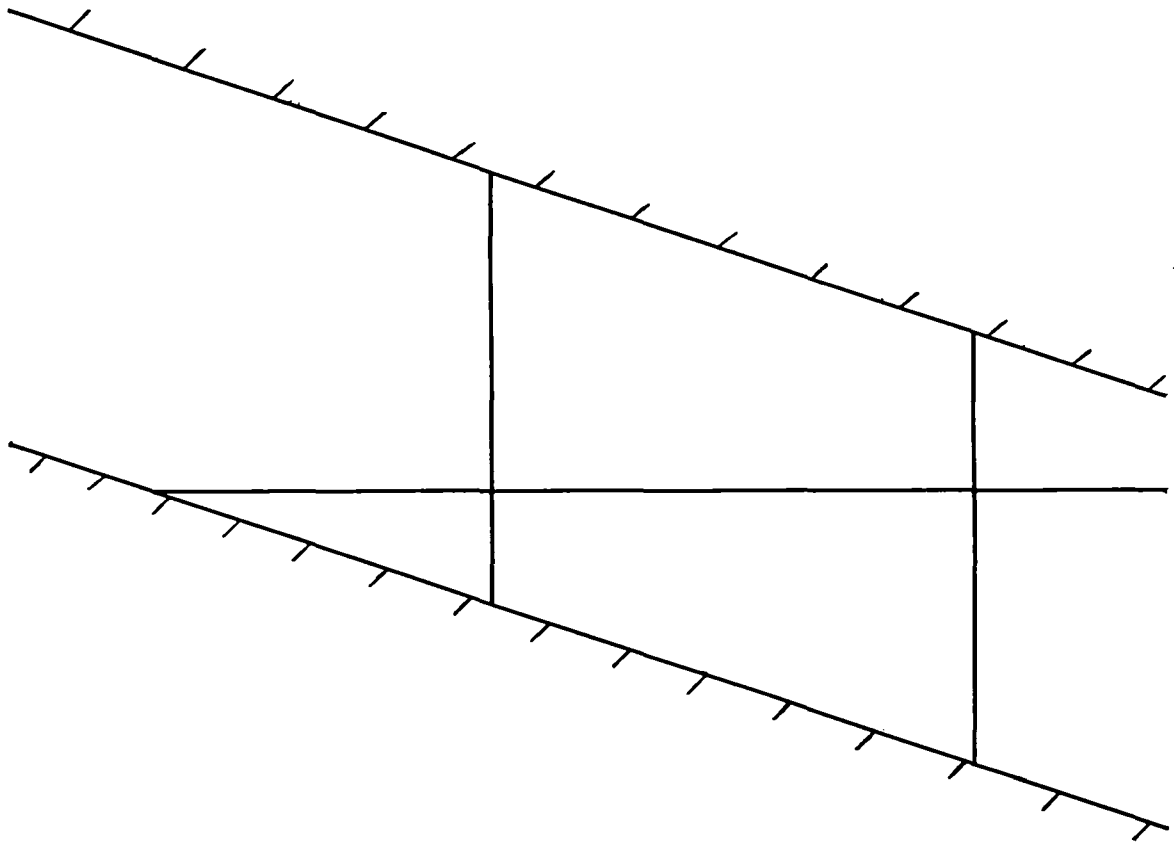


*Figure 21. Very Coarse Mesh*

## REFERENCES

1. Reyhner, T. A., "Computation of Transonic Potential Flow About Three-Dimensional Inlets, Ducts, and Bodies," NASA CR-3514, March 1982.
2. Reyhner, T. A., "Transonic Potential Flow Computation About Three-Dimensional Inlets, Ducts, and Bodies," AIAA Journal, Vol. 19, September 1981, pp. 1112-1121.
3. Brandt, A., "Multilevel Adaptive Computations in Fluid Dynamics," AIAA Journal, Vol. 18, October 1980, pp. 1165-1172.
4. McCarthy, D. R. and Reyhner, T. A., "Multigrid Code for Three-Dimensional Transonic Potential Flow About Inlets," AIAA Journal, vol. 20, January 1982, pp. 45-50.
5. "Experimental Data Base for Computer Program Assessment," AGARD-AR-138, 1979.
6. Carlson, J. R. and Compton, W. B. III, "An Experimental Investigation of Nacelle-Pylon Installation on an Unswept Wing at Subsonic and Transonic Speeds," NASA TP 2246, February 1984.
7. Gibson, S. G., "User's Manual for MASTER: Modeling of Aerodynamic Surfaces By Three-Dimensional Explicit Representation," NASA CR-166056, January 1983.

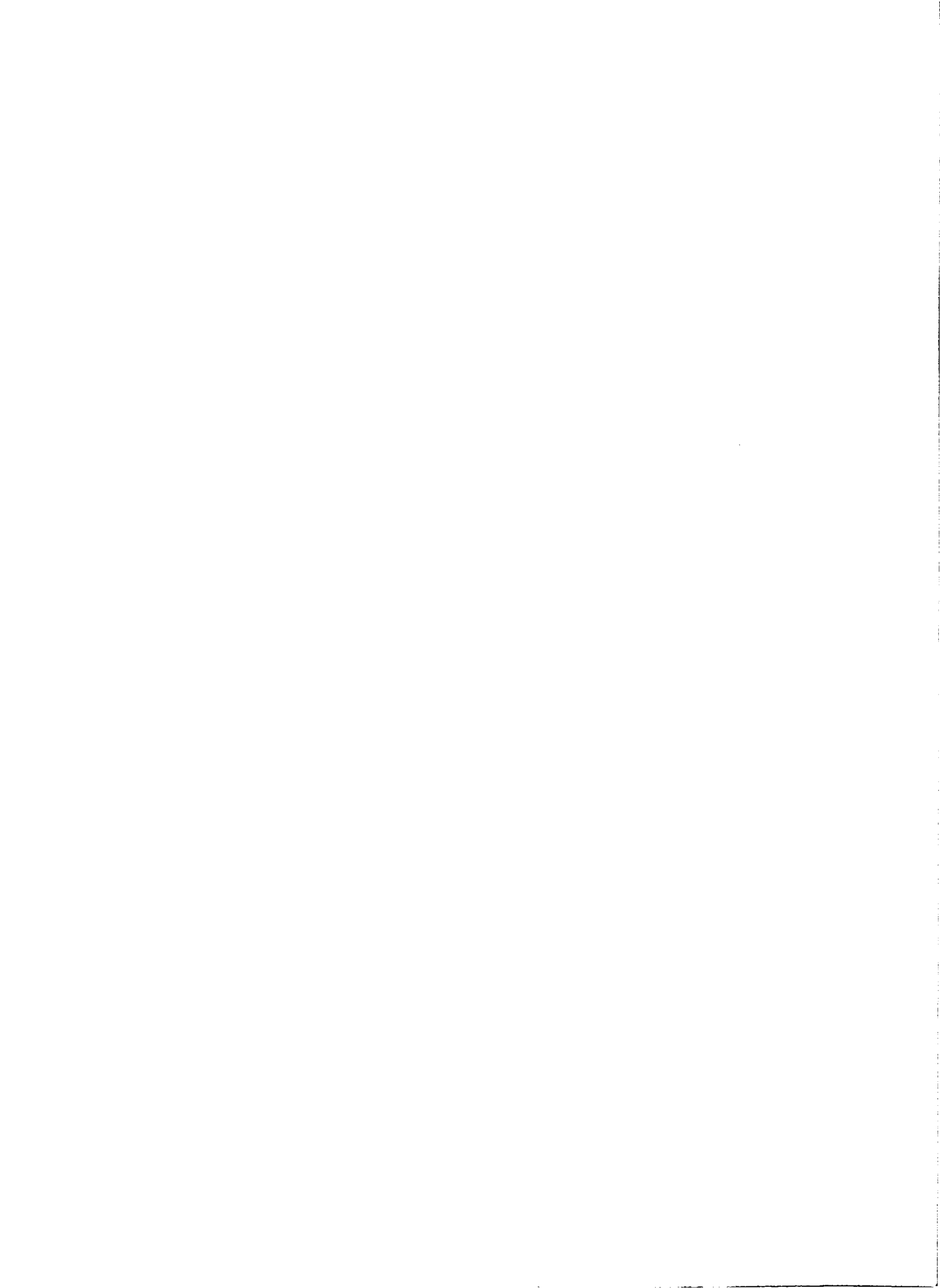








1. Report No. NASA CR-3814	2. Government Accession No.	3. Recipient's Catalog No.	
4. Title and Subtitle Three-Dimensional Transonic Potential Flow About Complex Three-Dimensional Configurations		5. Report Date July 1984	
		6. Performing Organization Code	
7. Author(s) Theodore A. Reyhner		8. Performing Organization Report No. D6-52329	
9. Performing Organization Name and Address Boeing Commercial Airplane Company P.O. Box 3707 Seattle, WA 98124		10. Work Unit No.	
		11. Contract or Grant No.	
		13. Type of Report and Period Covered Contractor Report	
12. Sponsoring Agency Name and Address National Aeronautics and Space Administration Washington, DC 20546		14. Sponsoring Agency Code	
15. Supplementary Notes Langley Technical Monitor: David E. Reubush Cooperative Agreement			
16. Abstract  An analysis has been developed and a computer code written to predict three-dimensional subsonic or transonic potential flow fields about lifting or nonlifting configurations. Possible configurations include inlets, nacelles, nacelles with ground planes, S-ducts, turboprop nacelles, wings, and wing-pylon-nacelle combinations. The solution of the full partial differential equation for compressible potential flow written in terms of a velocity potential is obtained using finite differences, line relaxation, and multigrid. The analysis uses either a cylindrical or Cartesian coordinate system. The computational mesh is not body fitted. The analysis has been programmed in FORTRAN for both the CDC CYBER 203 and the CRAY-1 computers. Comparisons of computed results with experimental measurement are presented. Descriptions of the program input and output formats are included.			
17. Key Words (Suggested by Author(s)) Transonic flow                      Inlets Inviscid flow                        Nacelles Potential flow                        Finite Three-dimensional flow            differences Multigrid                                Wings		18. Distribution Statement  Unclassified - Unlimited  Subject Category 02	
19. Security Classif. (of this report) Unclassified	20. Security Classif. (of this page) Unclassified	21. No. of Pages 77	22. Price A04



National Aeronautics and  
Space Administration

Washington, D.C.  
20546

Official Business

Penalty for Private Use, \$300

THIRD-CLASS BULK RATE

Postage and Fees Paid  
National Aeronautics and  
Space Administration  
NASA-451



**NASA**

POSTMASTER: If Undeliverable (Section 158  
Postal Manual) Do Not Return

---